Dyes and Pigments 90 (2011) 146–162

Contents lists available at ScienceDirect

Dyes and Pigments

journal homepage: www.elsevier.com/locate/dyepig

Steric and substituent control on the photoreversibility of some novel N-alkyl-3,3′-disubstituted-6-nitro-indolospirobenzopyrans: Evaluation using UV spectroscopic studies

Craig J. Roxburgh [a,*], Peter G. Sammes [b], Ayse Abdullah [b]

[a] Department of Chemistry, The Christopher Ingold Laboratories, University College, The University of London, London WC1H OAJ, UK
[b] Department of Chemistry, Surrey University, Guildford, GU2 7XH, UK

ARTICLE INFO

Article history:
Received 8 June 2010
Received in revised form
12 October 2010
Accepted 15 October 2010
Available online 23 October 2010

Keywords:
6-Nitro-spirobenzopyrans
Photoreversible
Colourisation (k_2) and decolourisation (k_1) rates
Equilibrium constants (K)
Substituent control
UV spectroscopy

ABSTRACT

A series of novel 6-nitro substituted indolospirobenzopyrans are reported. The effects of substitution on their photoreversibility are investigated by: synthesising derivatives that possess sterically hindering (with regard to the spiropyran-opening ↔ closing) groups contained within the spirocyclic skeleton. Specifically, spirobenzopyrans possessing combinations of various N-alkyl, and/or, simultaneously, 3,3′-geminal methyl and/or cyclohexyl groups are synthesised. Further, these systems are evaluated in three solvents; methanol, acetonitrile and dichloroethane. The thermal decolourisation rates of the *gem*-dimethyl and 3,3′-cyclohexyl compounds are additionally evaluated at the temperature of 50 °C. The above systems, and changes in physical parameters are extensively evaluated, and the subsequent biasing of the equilibria established using UV spectroscopy. Rates of colourisation, decolourisation and the equilibrium constants are obtained. The overall photochromic 'tuneability' of these systems is subsequently established.

1. Introduction

There is ongoing interest in the development of reversible metal-chelating agents in which chelation can be switched on-and off-by exposure to light of different wavelengths [1]. Several research groups have made notable contributions in this area [2]. A popular substrate for such studies is the 6-nitrospiro[1-benzopyran-2,2′-indole] system (**1a**) and its analogues since these have well-documented photochemical properties [3]. Photoirradiation with UV light at $\sim\lambda = 380$ nm leads to the ring-opened zwitterionic (merocyanine) form (**1b**), which can be converted back to the ring-closed form either by photoirradiation with visible light ($\sim\lambda = 550$ nm) or thermally Fig. 1. These photocolouration-thermodecolouration, or photocolouration-photodecolourisation cycles may be repeated between 5–10,000 times-depending on the specific type of system and have thus formed the basis of robust light-induced ionic switches. Further use of spirobenzopyrans, in particular, the photoreversible chelation of specific metal-ions has been reported in other systems [4–7]. Some elegant work utilising the Gd^{3+} ion has been reported by Sakata *et al.* [8]. Finally, it is important to emphasise the substantial contribution that the solvent [9] and substituents [10–12] exert on the ring-opening–closing reaction kinetics in spirobenzopyrans.

We have previously reported that the open ↔ closed dynamic equilibrium, an inherent property of spirobenzopyrans, under both dark conditions and photolysis could be greatly influenced by the use of appropriately placed electronically-influencing substituents. This was specifically the case when substituted in the 5-position of the indole-ring [13–15]; and also alkyl with alkyl-substituents placed in selected parts of the spirobenzopyran skeleton, including the alkenic-bond of the pyran ring [16]. Additionally, appropriately substituted spirobenzopyrans have been used to selectively transport ions across solvent interfaces, and that selectively placed skeletal substituents can be used to exert control over the process [17]. We now report the synthesis of a series of novel indolobenzospiropyrans containing combinations of N-alkyl, 3,3′-dialkyl and 6-nitro-substituents; and subsequently studies of the dynamic ring-opening ↔ closing rates of reaction within these systems by UV spectroscopy.

* Corresponding author. Present address: The Institute of Naval Medicine, Alverstoke, Gosport, Hants PO12 2DL, UK.
E-mail address: INM-EMS-OccHygSCRL@mob.uk (C.J. Roxburgh).

0143-7208/$ – see front matter © 2010 Elsevier Ltd. All rights reserved.
doi:10.1016/j.dyepig.2010.10.006

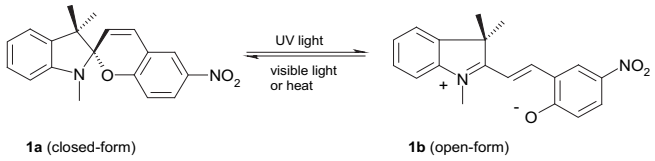

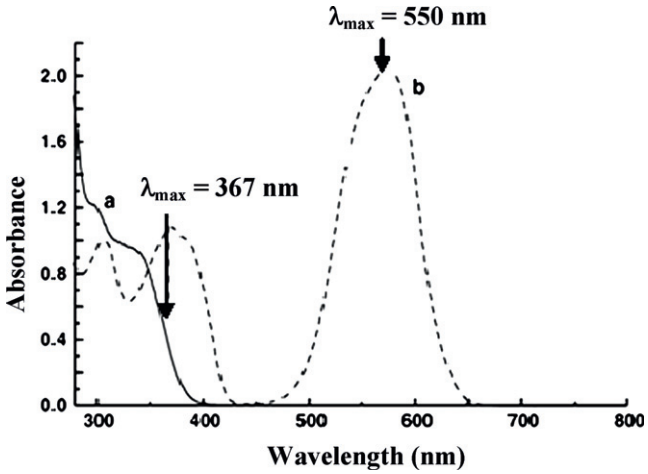

Fig. 1. Typical UV–VIS Absorption Spectra of the closed-(**1a**), and open-(**1b**) Indolospirobenzopyrans.

2. Results and discussion

2.1. Syntheses of indolobenzospiropyrans 2–5

The syntheses of the N-alkylindolospiropyrans **2**–**5** were undertaken using standard synthetic methods, or slight modifications thereof. Typically, the appropriately substituted alkyl-and aryl-hydrazines and ketones were condensed together to yield the corresponding hydrazones (*cf.* **7**) which were then cyclised to the indoles (*cf.* **10**) using the Fischer indole synthesis, and variations thereof. N-alkylation of the indoles was affected using various appropriate alkylating agents, from which the indolenines (*cf.* **8**) were obtained, after treatment with aqueous sodium hydroxide. The final indolospirobenzopyrans were obtained in good to excellent yields-ranging from 55 to 89%-by a condensation reaction between the appropriate indolenines and salicaldehydes in refluxing ethanol: typically, the reactions had gone to completion within a 24 h time period.

A 'general' synthesis is exemplified below, in Scheme 1, for the new N-hexyl-3,3′-cyclohexyl-substituted spirocyclic system **5**.

2.2. Kinetics and thermodynamic treatment of the reversible interconversion of the trans-merocyanine form. Variable temperature studies using UV spectroscopy

The kinetics of the spirobenzopyran ring-opening ↔ closing reaction have been described in several publications, [18–20] however there are no specific reports detailing the effects on the kinetics of this process where the spirobenzopran skeleton is substituted with various N-hexyl and/or electronically biasing functional groups—as depicted above (note: propyl- and phenyl- substituents in the 1-, 2- and 5-positions of spirobenzopyrans have been reported [21]). We have therefore studied, and report herein, the effects that these types of substitutions have on the benzospiropyran ring-opening ↔ closing reactions, and their corresponding reaction rates (Fig. 2).

Whilst the initial ring-opening reaction of the spirobenzopyrans is a relatively simple unimolecular reaction involving cleavage of the

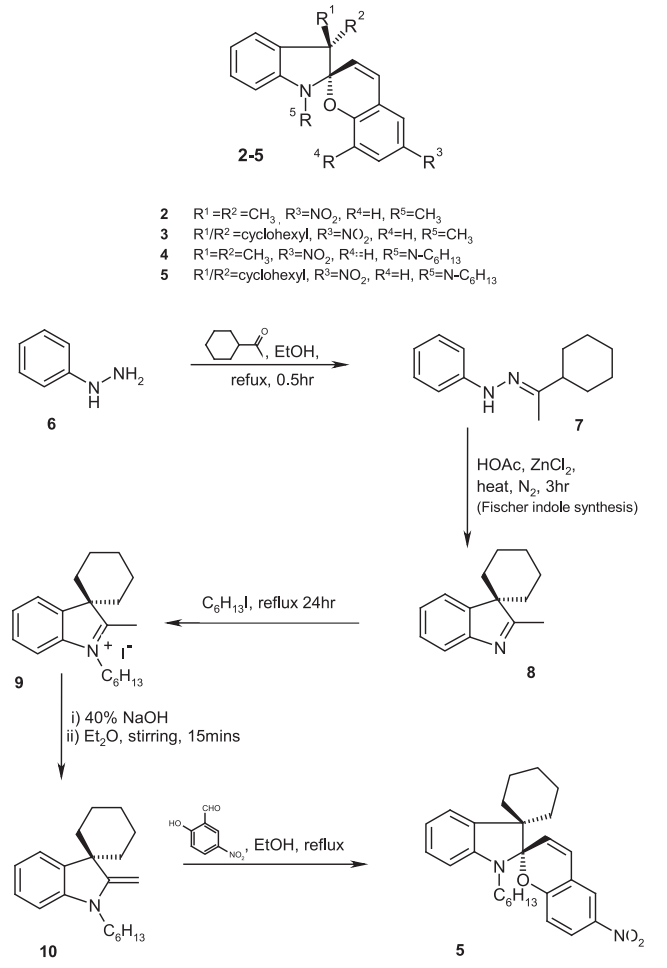

Scheme 1. N′-Hexyl-6-nitro-3′-spirocyclohexylspiro-[2*H*-1-benzopyran-2,2′-indoline] **5** (typical synthetic procedure used for compounds **2**-**5**).

spirocyclic carbon-oxygen bond, the open-merocyanine form is complex, existing as a potential mixture of eight different *cisoid*-and *transoid*-stereoisomers (Fig. 3). Therefore, the overall observed ring-closure rate is comprised of the sum of the individual isomer's ring-closure rates. However, at the final transition stage of ring-closure, there can only be the one *cisoid*-stereoisomer which closes to form the spirocyclic structure. Clearly, some stereoisomers are more thermodynamically stable than others, and at any given temperature there will be a significant predominance of one or more

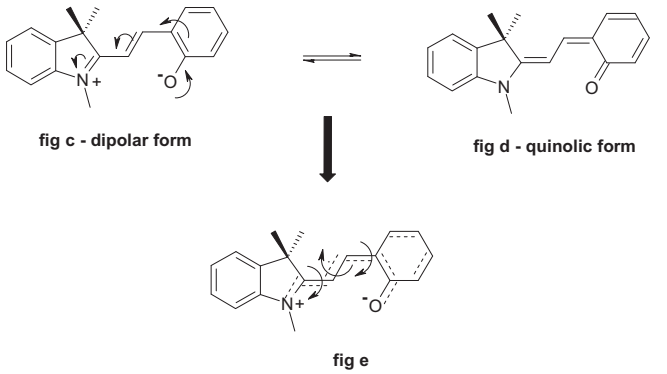

Fig. 2. Electronic distribution between the mesomeric forms of the *transoid*-photomerocyanine. (Conjugation between the two *trans*- merocyanine forms Fig 2c and Fig 2d allows rotation about the single bonds as depicted in Fig 2e).

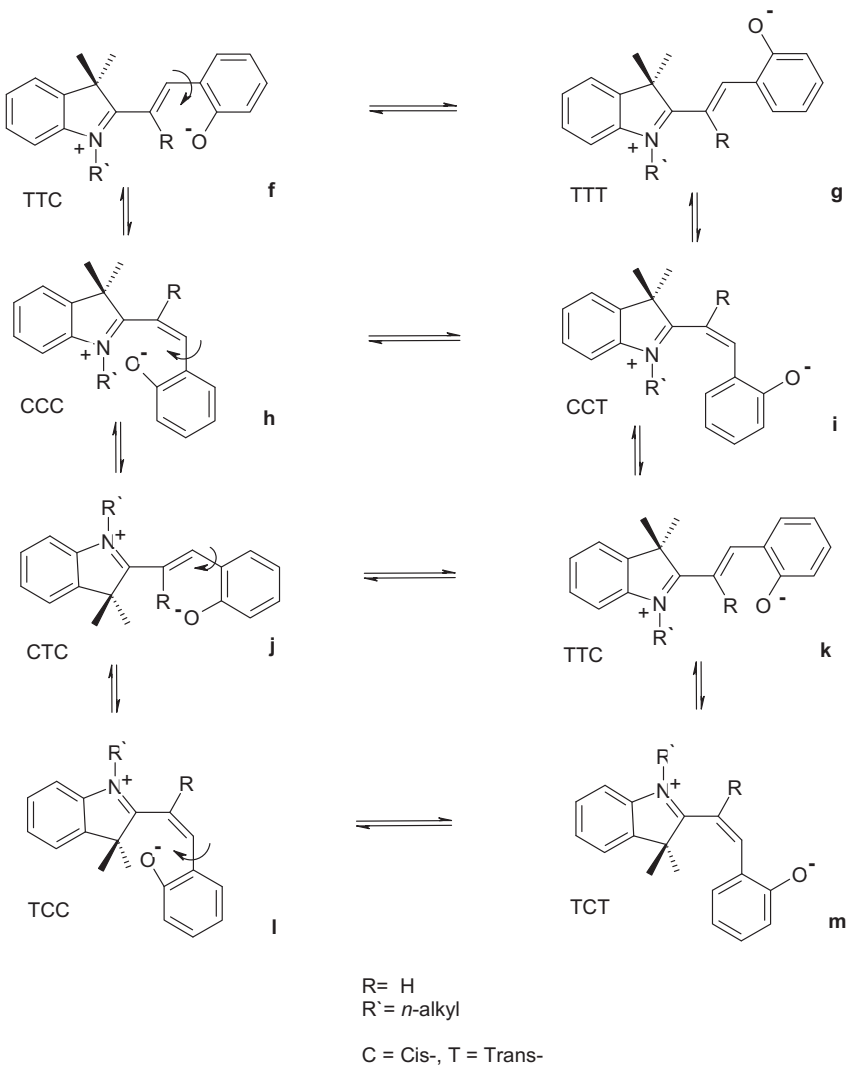

Fig. 3. The eight theoretically possible zwitterionic tautomeric isomers f-m of the open-form.

of them—in fact there is a predominant mixture of *trans*-isomers. Overall this is a very complex and multifactorial scenario the detailed discussion and analysis being outside the scope of this paper.

It is evident from the UV solution spectrum of spirobenzopyrans that the absorption peak present in the visible region (centered around $\lambda = 550$ nm), during the formation, or disappearance, of the *trans*-merocyanine form, increases or decreases respectively as the ring-opening ↔ closing process proceeds. This absorption peak has therefore been used as the reference wavelength with which to monitor the progress of these colourisation ↔ decolourisation reactions. Subsequently, a plot of absorbance at this particular wavelength—for the open-form—*vs*. time (*t*-in minutes) has been plotted for each of the various spirobenzopyran reactions studied. Since the concentration of the open-form (effectively formed *via* an *intra*-unimolecular reaction) can be taken as a first-order plot, a linear relationship should, theoretically, subsequently be obtained. For the colourisation reaction: calculation of the initial gradient, of the absorbance [A] *vs*. *t* graph allows the initial (init) rate of change in absorbance (which is directly proportional to the merocyanine form concentration change) allows calculation and comparisons of relative initial colourisation rates to be performed [The authors use the term k_{init} but stress that this is a relatively proportional measure of the initial rate of colourisation or decolourisation change and is not a formal rate constant]. The reverse process of decolourisation may be treated similarly; the initial rate of the absorption *vs*. time graph being proportional to the initial rate of decolourisation (k_{init}). Further, measurement of the gradient of the plot of 'ln[A−A_t] *vs*. time (t) enables the decolourisation rate to be established—this is defined here as the apparent rate constant (k_1) (whereby A is the initial absorbance, and A_t the absorbance at a time (t)). Similarly, the reverse is true, for the colourisation reaction, but in this case the plot would be ln[A_t−A] *vs*. time—also giving an apparent rate constant, defined here as k_2. Thus, as k_2/k_1 represents the equilibrium constant (K), the overall equilibrium position of these systems (depicted below) can be calculated (Table 5).

The half-lifes ($t_{1/2}$) for the reactions are obtained in the standard manner from the absorbance *vs*. time graphs (*i.e*. the time between any two points 'in time' over which the absorbance value has either halved, or doubled).

Lastly, by varying the temperature and subjecting the UV absorption data to the methods described above allows an indication of the equilibrium position, and thus the thermal stability at this particular temperature, to be obtained. The reactions of the spirobenzopyrans were additionally studied in three typical solvents (dichloroethane (DCE), acetonitrile and methanol) which provided further important information and how the medium could

potentially be utilised to influence their solution equilibria. This is particularly important when considering the design and practical operational efficiency of solution-based ion-chelating systems.

Overall, the above enables one to understand and quantify the effects that various alkyl-group substitutions exert on the spirobenzopyran ring-opening ↔ closing equilibria, associated solvent, and temperature effects. Subsequently, this enables one to predict the effects that these substitutions will exert on the photochromicity of spirobenzopyrans, which in turn permits application in the design of clean, or 'tuneable', on ↔ off photo-activated ionic switches, and selective ion-chelating systems.

2.3. Thermal decolourisation of compounds **2** and **3**

The thermal decolouration reaction of compounds **2** and **3**, at concentrations of 2×10^{-4} M, were studied in the three solvents detailed above, and at various temperatures (below), after irradiating with UV light for 1 min. Post irradiation, absorbance, due to the merocyanine structure, was continuously measured against time and the appropriate graphs plotted (Graphs 1–6).

The thermal decolourisation rates (k_1) for the compounds **2** and **3** at 2×10^{-4} M in acetonitrile, at a temperature of 21 °C, were calculated from gradients of the log graph *i.e.* graph 2, and the half-lifes ($t_{1/2}$) calculated from Graph 1. The calculated colourisation rates of reaction for compounds **2** and **3** from the graphs above are: $k_1 = 4.2 \times 10^{-1}$ min^{-1} and $k_1 = 7.1 \times 10^{-1}$ min^{-1} respectively; and the half-lifes ($t_{1/2}$) = 1 min and ($t_{1/2}$) = 2 min respectively.

Thermal decolourisation rate for compound **2** and compound **3** in acetonitrile at 2×10^{-4} M and at 21 °C.

Compound **3**			Compound **2**		
t (min)	Open-form absorbance at 550 nm	Ln A	*t* (min)	Open-form absorbance at 550 nm	Ln A
Dark					
0	0.81	−0.21072	0	0.746	−0.29303
0.5	0.547	−0.60331	0.5	0.618	−0.48127
1	0.386	−0.95192	1	0.508	−0.67727
1.5	0.277	−1.28374	1.5	0.405	−0.90387
2	0.204	−1.58964	2	0.325	−1.12393
2.5	0.155	−1.86433	2.5	0.263	−1.33560
3	0.122	−2.10373	3	0.216	−1.53248
3.5	0.1	−2.30259	3.5	0.180	−1.71480
4	0.085	−2.4651	4	0.152	−1.88387
4.5	<0.02		4.5	0.131	−2.03256
5	<0.02		5	0.115	−2.16282
			5.5	0.103	−2.27303
			6	0.094	−2.36446
			6.5	0.087	−2.44185
			7	<0.02	

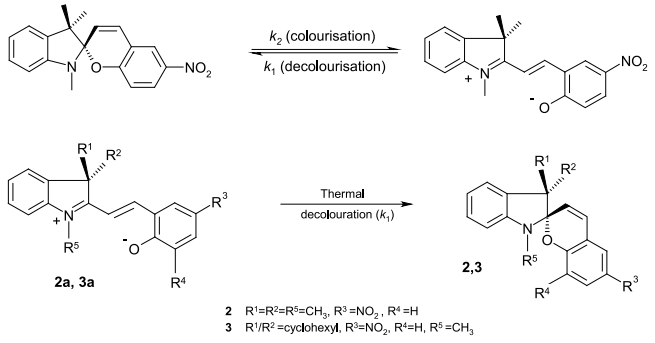

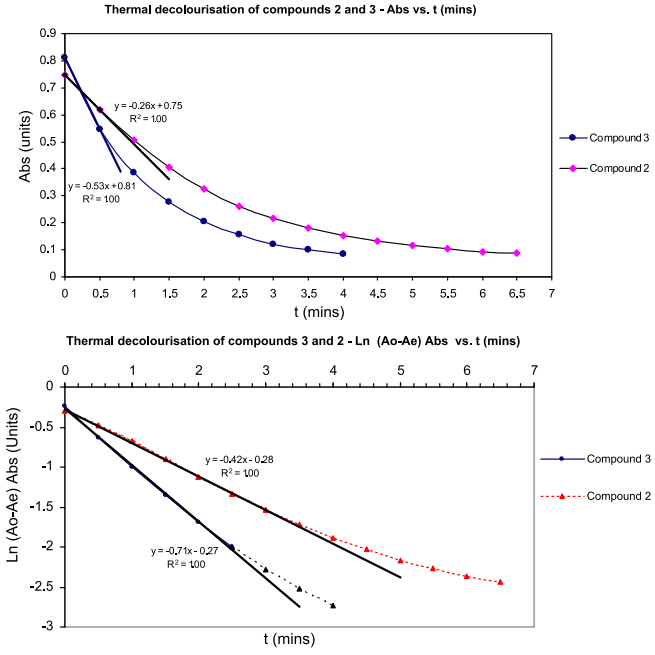

Graphs 1–2. Thermal decolourisation (Graph 1), and log absorbance (Graph 2) of compounds **2** and **3** in acetonitrile at a concentration of 2×10^{-4} M at 21 °C against time.

The above experiments were repeated at 21 °C in DCE and the resulting graphs reproduced below.

Lastly the above experiments were repeated at 21 °C in methanol and the resulting plots reproduced below.

The kinetic data is reproduced in Table 1 to facilitate immediate comparison of the data obtained, and the ensuing discussion.

The variation of thermal decolourisation rates (k_1) in the three solvents were compared and contrasted by plotting graphs of k_1 against: 1), acetonitrile; 2), DCE and 3), methanol (below) for both compounds **2** and **3** respectively. The Burdick and Jackson reference polarity (dielectric) index for organic solvents quotes values for acetonitrile, DCE and methanol of: 5.8, 3.5 and 5.1 respectively [22].

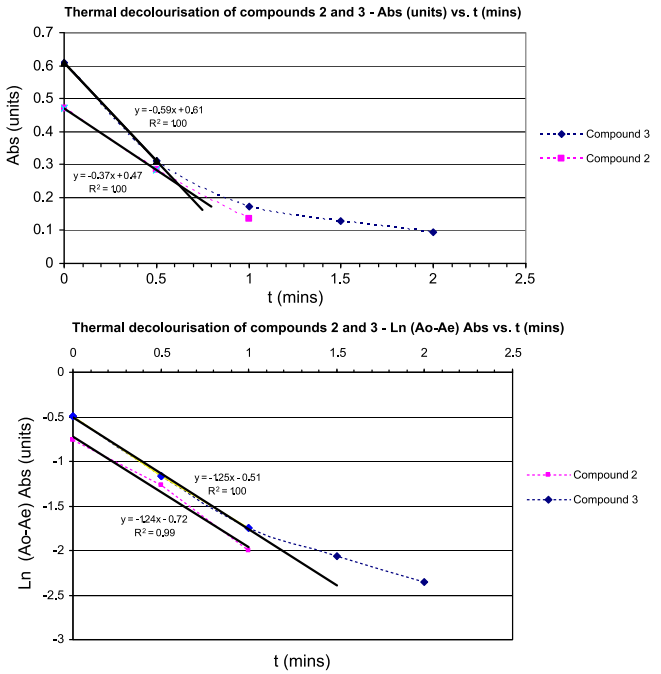

Graphs 3–4. Thermal decolourisation (Graph 3), and log absorbance (Graph 4) of compounds 2 and 3 in DCE at a concentration of 2×10^{-4} M at 21 °C against time.

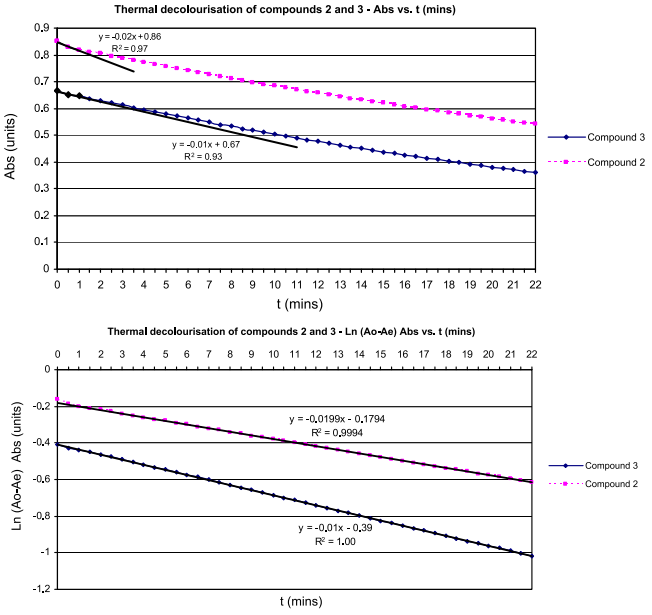

Graphs 5–6. Thermal decolourisation (Graph 5), and log absorbance (Graph 6) of compounds 2 and 3 in methanol at a concentration of 2×10^{-4} M at 21 °C against time.

Whilst the polarity of the solvents would be expected to play a significant part in influencing the equilibrium position of the spirobenzopyran ring-opening ↔ closing reaction, due to stabilization of the zwitterionic form, this is not the only important physical factor. The ability of the solvent to hydrogen bond, particularly to the merocyanine phenoxide ion, would possibly be at least as important, and probably more so. Additionally, the ability of the iminium ion to form a partial ion-pair bond (*i.e.* $=N^+ \leftrightarrow X\delta^-$(X = an electronegative atom) or $=N^+ \leftrightarrow$ lone pair) results in this moiety being capable of bonding to solvent atoms possessing a $\delta^- - \delta^+$ dipole-element, and/or a lone pair such as a nitrogen atom (*cf.* acetonitrile), or an oxygen atom (*cf.* methanol). Therefore, overall, it is likely that a combination of these major factors, and probably other parameters, will play a significant role in influencing and dictating the spirobenzopyran ↔ merocyanine equilibrium constants-which are in addition to the substituent effects (Graph 7).

Table 1
Summary of kinetic data for compounds **2** and **3** in acetonitrile, DCE and methanol at 21 °C at concentrations of 1×10^{-4} M.

Kinetic Data for compounds **2** and **3** in acetonitrile, DCE and methanol at 21 °C			
Structure	Solvent	k_1 (min^{-1})	Half-life ($t_{1/2}$)-min
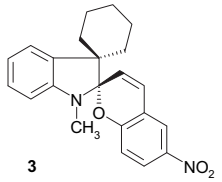 **3**	CH_3CN	7.1×10^{-1}	1
	DCE	1.25	0.5
	MeOH	1.0×10^{-2}	509.7 (Calc'd)
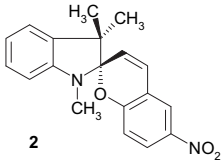 **2**	CH_3CN	4.2×10^{-1}	2
	DCE	1.24	0.65
	MeOH	2×10^{-2}	49.51 (Calc'd)

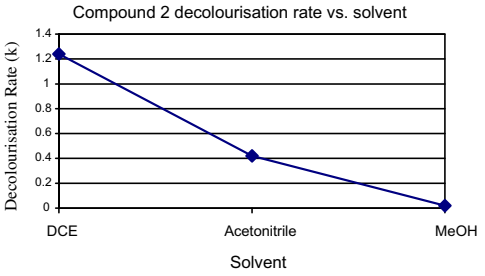

Graph 7. Rates of thermal decolourisation (k_1) for compound **2** in DCE, acetonitrile and methanol solvents.

In summary, at a concentration of 2×10^{-4} M, and at 21 °C, some clear trends in the rates of thermal decolourisations (k_1) for compounds **2** and **3** are realized. This is clearly evident when examining the above decolourisation rate (k_1) *vs.* solvent plots.

For compound **2** the rate of thermal decolourisation varies considerably with solvent. The fastest rate of decolourisation occurs in the least polar solvent (DCE: polarity = 3.5) and is almost 3 times faster than in acetonitrile (polarity = 5.8). This result is perhaps not surprising since the rate of decolourisation is partly dependent on the degree of stability exerted on the zwitterionic form by the solvent. Acetonitrile being considerably more polar than DCE 'solution-stabilizes' the open-form considerably more than DCE by restricting and consequently slowing cyclisation. Significantly reduced interactions are expected in a relatively 'inert' solvent, such as DCE, consequently relatively uninhibiting cyclisation. When observing the thermal re-cyclisation in methanol a significant reduction in rate is noted. Whilst the reference polarity reported for methanol is 5.1, which is similar to that of acetonitrile, the relative rate of thermal decolourisation is just 0.02 s^{-1}-21 times lower—the largest relative difference between all three solvents. This observation is perhaps not surprising since methanol is additionally able to stabilize the open form through hydrogen bonding, around both the phenoxide and iminium ions.

Consideration of compound **3** reveals a similar relative trend in thermal decolourisation rates to those observed for **2**, although as expected, with a difference in absolute values. These differences in absolute values, obviously arising from the differing functional group substitutions, are discussed below.

Comparing and contrasting compounds **2** and **3**: the rates of thermal decolourisation (k_1) for compound **3** is greater than that of **2** in CH_3CN and DCE, but to significantly differing degrees. The largest difference (a factor of ~1.7 times (0.71 s^{-1}/0.4 min^{-1})-and a relative difference of ~0.3 min^{-1}) is recorded in acetonitrile with the difference in DCE being negligible (1.25 min^{-1} *vs.* 1.24 min^{-1}). This would indicate, in the absence of solvent effects—or at least the relatively minimal ones that would be expected to occur in DCE—that the thermal decolourisation rates of these two compounds are almost identical, with **3** possessing a modestly greater rate (1.25 min^{-1} *vs.* 1.24 min^{-1}). Therefore the indications are that in this solvent, and at the given temperature, the ring-closing reaction is similarly biased for both *gem*-dimethyl and 3,3′-cyclohexyl-substituted spirobenzopyrans. Additionally, as the fastest rate of decolourisation for the merocyanines is in the least polar solvent (DCE); this would indicate less polar solvation and hence less stabilization of the merocyanine Zwitterion is occurring (a more polar solvent would have greater ability to solvate the Zwitterion-stabilizing it-and consequently reducing its rate of decolourisation). It is of note that the initial decolourisation rates (k_{init}) are almost identical the overall decolourisation rate (k_1), and consequently the reverse reaction rate (colourisation) (k_2) is near to zero (within decimal place rounding). This indicates a very slow decolourisation

reaction with almost insignificant colourisation reaction occurring: calculated half-lifes of ~50 min for compound **2** and 510 min for compound **3** would support this (Graph 8).

Thermal decolourisation rate for compound **3** and compound **2** in DCE at 2×10^{-4} M and at 21 °C.

Compound **3**			Compound **2**		
Dark *t* (min)	Open-form absorbance at 550 nm	Ln A	Dark *t* (min)	Open-form absorbance at 550 nm	Ln A
0	0.608	−0.49758	0	0.47	−0.75502
0.5	0.311	−1.16796	0.5	0.283	−1.26231
1	0.174	−1.7487	1	0.136	−1.9951
1.5	0.127	−2.06357	1.5		
2	0.095	−2.35388	2		
2.5			2.5		
3			3		

However, in acetonitrile **3** undergoes thermal decolourisation ($k_1 = 0.71$ min^{-1}) at ~1.7 times the rate of **2** ($k_1 = 0.42$ min^{-1}) indicating a relatively less thermally stable merocyanine form. Thus, in this case, with merocyanine possessing a bulky 3,3′-cyclohexyl-grouping, solvent effects appear to be operating. Any polar solvent interactions are expected to be maximally centered around the phenoxide and iminium ions. For both compounds **2** and **3** solvent interactions around the phenoxide ions are expected to be similar (as they are sterically similarly available), however differences would be expected to arise around the iminium ions since **3** possesses a nearby sterically bulky 3,3′-cyclohexyl group, as opposed to **2** possessing a *gem*-dimethyl group. Differences in solvation around the iminium ion, and consequently the merocyanine form, are therefore expected and hence probably a major cause of the differing thermal decolourisation rates.

The largest changes in decolourisation rates (k_1) occur in methanol where they significantly reduce *i.e.* in the case of compound **3** k_1 is 125 times slower than in DCE (and 71 times slower in acetonitrile); and in the case compound **2** 62 times slower (and 21 times slower in acetonitrile). The lower polarity of methanol (5.1) than acetonitrile (5.8) is contrary to a concomitantly lower decolourisation rate and cannot alone explain this significant reduction. In this case it is expected that methanol, which possesses significant hydrogen bonding capability, hydrogen bonds to the phenoxide ion greatly inhibiting ring-closure. Additionally, the oxygen lone-pairs of methanol can coordinate towards the iminium ion, which offers further stabilization, limiting the ability to re-cyclise (decolourise). The above explains why the decolourisation rates are significantly lower in methanol-likely to be so in other polar solvents—and increasingly so in ones that can additionally

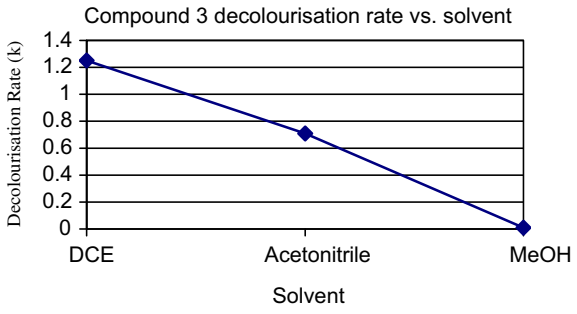

Graph 8. Rates of thermal decolourisation (k_1) for compound **3** in DCE, acetonitrile and methanol solvents.

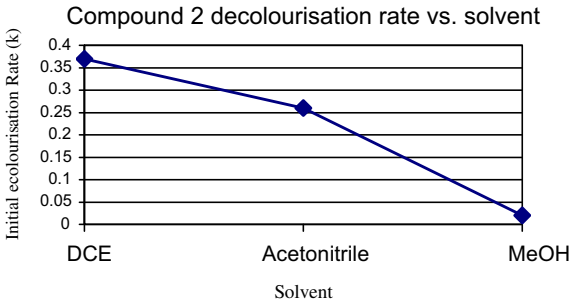

Graph 9. Initial (init) rates of thermal decolourisation (k_{init}) for compound **2** in DCE, acetonitrile and methanol solvents.

hydrogen bond. Lastly, the fact that the rates of thermal decolourisation for compounds **2** and **3** are of a similar magnitude is perhaps surprising. It is possible that the effects discussed above produce a thermal energy leveling effect between the compounds at this temperature, largely negating steric/substituent effects, which explains why their rates are near parity.

It can be seen from the graphs of initial decolourisation rates (k_{init}) that these, to a degree, parallel those for the apparent decolourisation rates obtained from the log graphs. Some slight variations are noted, as might be expected. The initial decolourisation rates for compound **2** in DCE and acetonitrile are considerably less (almost 70% and 60% respectively) than the overall decolourisation rates (k_1), and do not undergo a similar magnitude drop in changing from DCE to acetonitrile solvents; the graph depicts an uplift rather than the observed dropdown. However, interestingly, both rates compare favorably when contrasted in methanol solvent. This indicates the significant influence on the ring-opening reaction exerted by the solvent. For compound **3** a similar trend is noted but the initial decolourisation rates drop by margins of 50% and 25% respectively. Similar to compound **2**, an uplift in initial decolourisation rate for compound **3** is also noted in acetonitrile, but in this case it is ~30% as opposed to almost 70%. Rates in methanol remained similarly low and mirrored the pattern observed for compound **2**. In summary, as might be expected, substituent effects substantially influence the initial decolourisation rates, except where solvent effects dominate, as is the case of methanol-through polarity and hydrogen bonding (Graph 9).

As extremely low thermal decolourisation reaction rates were observed in methanol at 21 °C, postulated to be due to significant solvent interactions, it was decided to investigate whether this could be biased, or at least alleviated by conducting the same experiments at a higher temperature (Graph 10). This increased temperature should reduce the transitional energy barrier to decolourisation. Additionally, reduction of these solvent interactions would potentially allow one to observe and study the important alkyl-substituent

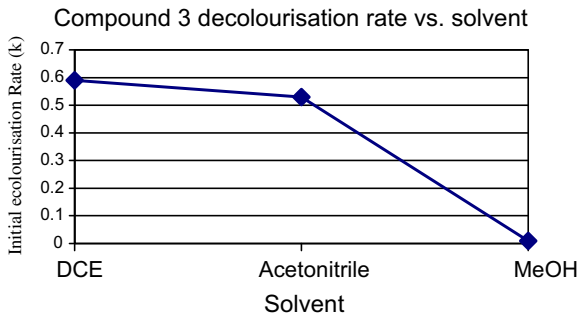

Graph 10. Initial rates of thermal decolourisation (k_{init}) for compound **3** in DCE, acetonitrile and methanol solvents.

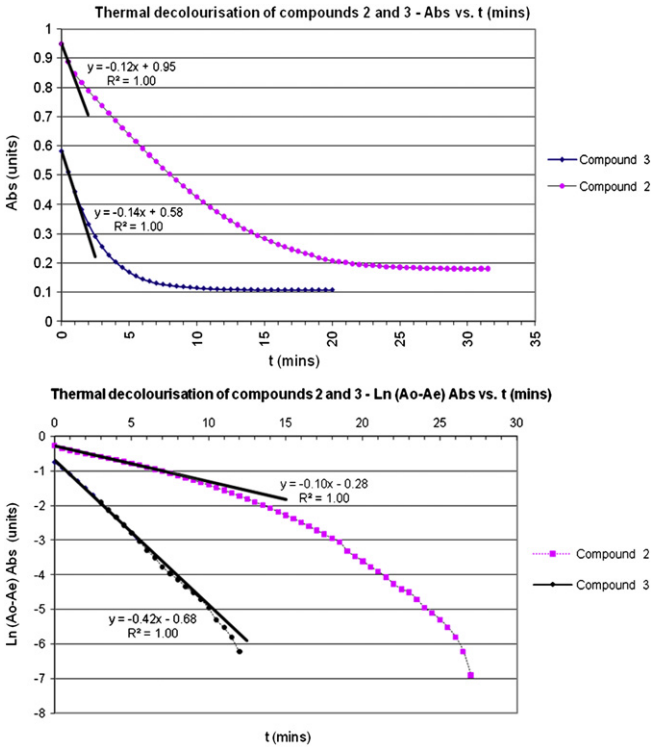

Graphs 11–12. Thermal decolourisation (Graph 11), and log absorbance (Graph 12) of compounds 2 and 3 in methanol at a concentration of 2×10^{-4} M at 50 °C against time.

effects that are known to operate in the spirobenzopyran ring-opening ↔ closing process. To this end we conducted the above experiments in methanol at a temperature of 50 °C calculating the thermal decolourisation rates utilizing Graphs 11 and 12. The results are subsequently summarized and compared to those obtained at 21 °C (Table 2).

Thermal decolourisation rate for compound **3** and compound **2** in MeOH at 2×10^{-4} M, and at 21 °C.

Compound **3**			Compound **2**		
Dark *t* (min)	Open-form absorbance at 550 nm	Ln A	Dark *t* (min)	Open-form absorbance at 550 nm	Ln A
0	0.665	−0.40797	0	0.85	−0.16252
0.5	0.651	−0.42925	0.5	0.829	−0.18754
1	0.646	−0.43696	1	0.818	−0.20089
1.5	0.637	−0.45099	1.5	0.810	−0.21072
2	0.629	−0.46362	2	0.804	−0.21816
2.5	0.621	−0.47642	2.5	0.795	−0.22941
3	0.612	−0.49102	3	0.787	−0.23953
3.5	0.604	−0.50418	3.5	0.779	−0.24974
4	0.596	−0.51751	4	0.771	−0.26007
4.5	0.587	−0.53273	4.5	0.763	−0.27050
5	0.579	−0.54645	5	0.756	−0.27971
5.5	0.571	−0.56037	5.5	0.748	−0.29035
6	0.563	−0.57448	6	0.741	−0.29975
6.5	0.556	−0.58699	6.5	0.733	−0.31061
7	0.548	−0.60148	7	0.726	−0.32021
7.5	0.54	−0.61619	7.5	0.719	−0.32989
8	0.533	−0.62923	8	0.711	−0.34108
8.5	0.525	−0.64436	8.5	0.705	−0.34956
9	0.518	−0.65778	9	0.696	−0.36241
9.5	0.511	−0.67139	9.5	0.691	−0.36962
10	0.504	−0.68518	10	0.684	−0.37980
10.5	0.497	−0.69917	10.5	0.677	−0.39008
11	0.49	−0.71335	11	0.671	−0.39899
11.5	0.483	−0.72447	11.5	0.664	−0.40947
12	0.477	−0.74024	12	0.659	−0.41703

(*continued*)

Compound **3**			Compound **2**		
Dark *t* (min)	Open-form absorbance at 550 nm	Ln A	Dark *t* (min)	Open-form absorbance at 550 nm	Ln A
12.5	0.47	−0.75502	12.5	0.657	−0.42007
13	0.463	−0.77003	13	0.645	−0.4385
13.5	0.457	−0.78307	13.5	0.638	−0.44942
14	0.451	−0.79629	14	0.632	−0.45887
14.5	0.445	−0.80968	14.5	0.626	−0.46840
15	0.438	−0.82554	15	0.620	−0.47804
15.5	0.432	−0.83933	15.5	0.614	−0.48776
16	0.426	−0.85332	16	0.607	−0.49923
16.5	0.42	−0.86750	16.5	0.602	−0.50750
17	0.415	−0.87948	17	0.596	−0.51751
17.5	0.409	−0.89404	17.5	0.590	−0.52763
18	0.404	−0.90634	18	0.584	−0.53785
18.5	0.398	−0.92130	18.5	0.579	−0.54645
19	0.392	−0.93649	19	0.573	−0.55687
19.5	0.387	−0.94933	19.5	0.567	−0.56740
20	0.382	−0.96233	20	0.562	−0.57625
20.5	0.377	−0.97551	20.5	0.557	−0.58519
21	0.372	−0.98886	21	0.551	−0.59602
21.5	0.367	−1.00239	21.5	0.547	−0.60331
22	0.362	−1.01611	22	0.541	−0.61434

Thermal decolourisation rate for compound **3** and compound **2** in MeOH at 2×10^{-4} M, and at 50 °C.

Compound **3**			Compound **2**		
Dark *t* (min)	Open-form absorbance at 550 nm	Ln A	Dark *t* (min)	Open-form absorbance at 550 nm	Ln A
0	0.582	−0.54128	0	0.949	−0.05235
0.5	0.51	−0.67334	0.5	0.885	−0.12217
1	0.443	−0.81419	1	0.846	−0.16723
1.5	0.383	−0.95972	1.5	0.817	−0.20212
2	0.333	−1.09961	2	0.788	−0.23826
2.5	0.291	−1.23443	2.5	0.763	−0.27050
3	0.256	−1.36258	3	0.737	−0.30517
3.5	0.227	−1.48281	3.5	0.712	−0.33968
4	0.204	−1.58964	4	0.687	−0.37542
4.5	0.185	−1.6874	4.5	0.662	−0.41249
5	0.169	−1.77786	5	0.638	−0.44942
5.5	0.156	−1.8579	5.5	0.615	−0.48613
6	0.145	−1.93102	6	0.591	−0.52594
6.5	0.138	−1.9805	6.5	0.568	−0.56563
7	0.131	−2.03256	7	0.546	−0.60514
7.5	0.127	−2.06357	7.5	0.524	−0.64626
8	0.124	−2.08747	8	0.503	−0.68717
8.5	0.121	−2.11196	8.5	0.483	−0.72774
9	0.119	−2.12863	9	0.463	−0.77003
9.5	0.117	−2.14558	9.5	0.444	−0.81193
10	0.115	−2.16282	10	0.426	−0.85332
10.5	0.113	−2.18037	10.5	0.408	−0.89649
11	0.112	−2.18926	11	0.391	−0.93905
11.5	0.111	−2.19823	11.5	0.375	−0.98083
12	0.110	−2.20727	12	0.359	−1.02443
12.5	0.110	−2.20727	12.5	0.345	−1.06421
13	0.110	−2.20727	13	0.331	−1.10564
13.5	0.109	−2.21641	13.5	0.318	−1.14570
14	0.109	−2.21641	14	0.306	−1.18417
14.5	0.108	−2.22562	14.5	0.294	−1.22418
15	0.108	−2.22562	15	0.283	−1.26231
15.5	0.108	−2.22562	15.5	0.274	−1.29463
16	0.108	−2.22562	16	0.264	−1.33181
16.5	0.108	−2.22562	16.5	0.255	−1.36649
17	0.108	−2.22562	17	0.247	−1.39837
17.5	0.108	−2.22562	17.5	0.240	−1.42712
18	0.108	−2.22562	18	0.233	−1.45672
18.5	0.108	−2.22562	18.5	0.228	−1.47841

(*continued*)

Compound **3**			Compound **2**		
Dark *t* (min)	Open-form absorbance at 550 nm	Ln A	Dark *t* (min)	Open-form absorbance at 550 nm	Ln A
19	0.108	−2.22562	19	0.217	−1.52786
19.5	0.108	−2.22562	19.5	0.212	−1.55117
20	0.108	−2.22562	20	0.208	−1.57022
			20.5	0.204	−1.58964
			21	0.203	−1.59455
			21.5	0.198	−1.61949
			22	0.195	−1.63476
			22.5	0.193	−1.64507
			23	0.192	−1.65026
			23.5	0.190	−1.66073
			24	0.188	−1.67131
			24.5	0.187	−1.67665
			25	0.186	−0.68201
			25.5	0.185	−1.68740
			26	0.184	−1.69282
			26.5	0.183	−1.69827
			27	0.182	−1.70375
			27.5	0.182	−1.70375
			28	0.182	−1.70375
			28.5	0.181	−1.70926
			29	0.181	−1.70926
			29.5	0.181	−1.79026
			30	0.180	−1.71480
			30.5	0.180	−1.71480
			31	0.181	−1.70926
			31.5	0.181	−1.70926

It is clear that raising the temperature produces three significant effects: 1) the initial rates of decolourisation (k_{init}) for compounds **3** and **2** are significantly higher—14 times (0.14 min^{-1} *vs.* 0.01 min^{-1}) and 6 times (0.12 min^{-1} *vs.* 0.02 min^{-1}) respectively, at 21 °C; 2) significantly higher thermal rate constants (k_1) for compounds **3** (0.42 min^{-1}) and **2** (0.1 min^{-1}) are noted at this temperature, as opposed to that at 21 °C (0.01 and 0.02 min^{-1} respectively). This calculates to 42 times (0.42 min^{-1}/0.01 min^{-1}) and 5 times (0.1 min^{-1}/0.02 min^{-1}) respectively; and 3) a significant difference in decolourisation rates (k_1) between the *gem*-dimethyl **2** (0.1 min^{-1}) and 3,3′-cyclohexyl **3** (0.42 min^{-1}) compounds (4.2 times (0.42 min^{-1}/0.1 min^{-1})) becomes apparent, highlighting the expected substituent effects that were not observed at the lower temperature. Further, the increased rate of decolourisation for the 3,3′-cyclohexyl substituted compound vindicates the fact that sterically bulky groups destabilize the open-zwitterionic form promoting ring-cyclisation. It is also apparent from Graph 12 that compound **2** possesses a slight 'hyperbolic' element. As discussed earlier, and particularly at this higher temperature, the merocyanine form can exist in a number of conformations. This results in the existence of several simultaneous ring-closure reactions-with their concomitant individual rate constants (fast and slow fading-rates)—potentially resulting in an apparent non-linear rate. In addition, there exists the possibility that one or more of the merocyanine rotamers possesses a longer half-life, also potentially contributing to the explanation of the 'hyperbolic-shaped' graph.

Further, these rate constant results are supported and enforced by the corresponding half-lives, which for compounds **2** and **3** are 8.75 ($k_1 = 1.0 \times 10^{-1}$ min^{-1}) and 2.5 ($k_1 = 4.2 \times 10^{-1}$ min^{-1}) min, respectively.

Overall the above findings will find useful practical implications in the design of 'tunable' photoreversible spirobenzopyran systems.

Additionally, by studying the same decolourisation reactions under identical physical conditions, but at two different temperatures, the activation energies (Ea's) of spirobenzopyran formation can be calculated using Eq (1):

$$\mathrm{Ln}(k_2/k_1) = -\Delta \mathrm{Ea}/\mathrm{R}[(1/\mathrm{T}_2) - (1/\mathrm{T}_1)] \quad (1)$$

R (gas constant) = 8.314 J mol^{-1} K^{-1}; $T = 21$ °C (294 K) and 50 °C (323 K); k_2 and k_1 are the decolourisation rate constants (s^{-1}) at the different temperatures (T) in Kelvin (K).

For compounds **2** and **3** the positive activation energies are 44 and 102 kJ mol^{-1} respectively. The relatively lower activation energy for **2**, as compared to **3** (a ratio of 2.3 times) indicates **2** is relatively more stable than **3**. This is probably due to lower steric strain operating in the closed-form of the *gem*-dimethyl compound as compared to the 3,3′-cyclohexyl analogue. Additionally, this supports, and closely parallels the observed relative increased rates of decolourisation values for the two compounds (described later) *i.e.* value of 0.19 s^{-1} for the 3,3′-cyclohexyl compound **3** as opposed to 0.02 s^{-1} for the *gem*-dimethyl-substituted compound **2**—a ratio of 9.5 times for the more highly substituted compound. Again, this is probably due to the greater relief in steric strain experienced by the more highly substituted compound-in undergoing ring-opening.

Lastly, the Gibbs free energy (G in kJ) for compounds **2**–**5** at 21 °C can be deduced from their calculated equilibrium constants (K) (Note: although the equilibrium constants are calculated later in this paper (Table 5) it is sensible to calculate and reproduce the Gibb's free energy values at this point) using Eq (2):

$$\ln K = -[\Delta G/RT] \quad (2)$$

R (gas constant) = 8.314 J mol^{-1} K^{-1}; T = 21°C (294 K) and 50 °C (323 K).

The calculated values for G (kJ) for compounds **2**–**5** are: −0.662; −3.036; 2.872 and 0.840 respectively. Examination of these values enables the following relative ease of colourisation reaction order to be established:

$$3 > 2 > 5 > 4$$

This order exactly parallels the calculated trend (described later) for the colourisation reaction equilibrium constants.

Table 2
Summary of kinetic data compounds for **2** and **3** in methanol at 50 °C.

Kinetic Data for Compounds **2** and **3** in methanol at 50 °C and 25 °C				
Structure	50 °C		25 °C	
	k_1 (min^{-1})	Half-life ($t_{1/2}$)-min	k_1 (min^{-1})	Half-life ($t_{1/2}$)-min
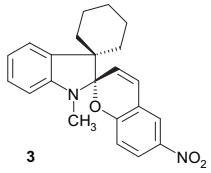 **3**	4.2×10^{-1}	2.5	1.0×10^{-2}	509.7 (Calc'd from Ln2/1.36 × 10^{-3})
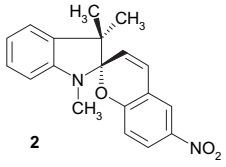 **2**	1.0×10^{-1}	8.75	2.0×10^{-2}	49.51 (Calc'd from Ln2/5.50 × 10^{-4})

Using these Gibb's free energy values we are also able to calculate the entropy of formation (S, J K^{-1}) for compounds **2** and **3** using the Eq (2):

$$\Delta G = \Delta H - T\Delta S \quad (3)$$

Values for the entropies of formation (J K^{-1}) for **2** and **3** at 21 °C are: 2060 and 4713 respectively. Therefore, formation of compound **3** is more than twice as entropically favorable as that of compound **2**, which is in line with the free energy of formation values.

2.4. N-Hexyl-3,3′-substituted-spirobenzopyrans

If a truly on ↔ off UV-activated switchable photochromic system is required then, in these structures, there exists a need for the development of systems with larger energy barriers between the various photoisomers. Therefore, photochromic systems possessing additional sterically bulky and hindering groups were examined in order to obtain an understanding of what effect these groups have on the ease of the ring-closing ↔ opening reaction. We therefore decided to turn our attention towards the investigation of a further two novel spirobenzopyrans **4** and **5**, which in addition to containing 3,3′-*gem*-dimethyl and 3,3′-cyclohexyl-groups, possessed the sterically bulky N-hexyl moiety. [It is noteworthy at this point to reference the important contribution made by Gabbutt and coworkers who synthesised a number of alternative N-alkyl-containing indolenine [23] intermediates, which were subsequently used to produce a variety of photochromic spiroindolinonaphthoxazines]. These were prepared in order to specifically investigate what effect the N-hexyl-group exerts on the rates of colourisation (k_2), decolourisation (k_1); and hence the resulting equilibrium constants (K). These new compounds were subsequently compared and contrasted against their structurally equivalent congeners—maintaining the same 3,3′-*gem*-dimethyl **2** or 3,3′-cyclohexyl-**3** substitution pattern-but possessing an N-methyl group. In order to undertake these comparisons a second set of thermal colourisation and decolourisation data sets, containing a similar number of data points, were experimentally obtained: These new data sets allowed a more practically convenient comparison. [Note: it was not practicable to record as many measurements in these experiments due to time constraints. This produced some difference in the values of k_1 as compared to those previously obtained when utilizing a far greater number of data points. However, this offered a better relative comparison]. The plots of absorption against time, for both the colourisation and decolourisation reactions, and subsequently the corresponding log rates against time, for compounds **2** and **3**, are thus revisited utilising these data sets. Similar data sets were also experimentally obtained for the N-hexyl-substituted compounds, which were subsequently subjected to the same graphical plots as those of the N-methyl-substituted compounds. The ensuing results for all four compounds, specifically; the rates of colourisation (k_2), decolourisation (k_1), and calculated equilibrium constants (K), were compared and contrasted. Some significant trends are observed which are subsequently graphically represented *via*- scatter plots.

Firstly, the thermal colourisation reactions of compounds **2**, **3**, **4** and **5** in methanol at 21 °C, and a concentration of 2×10^{-4} M were considered. The data for the thermal colourisation reactions are summarized below in Table 3.

Examination of the thermal log rate colourisation graphs indicate some deviation from linearity (overall the correlation coefficients display values in the range of 0.94 to ~0.99). This indicates that a more complex (not a simple unimolecular spirocyclic ring-opening) scenario is operating. The thermal colourisation process involves initial cleavage of the spirocyclic carbon-oxygen bond 'eventually' generating the *trans*-merocyanine structure depicted in Fig. 2c;-all linking bonds being *trans(t)*–[16] *i.e.* (*t,t,t*) (Note: In practice, the real structure will have relative partial, and opposite charges (δ^+ and δ^-) localised on the indolium-nitrogen and phenolic-oxygen atoms, respectively). Electronic conjugation between the dipolar zwitterionic (Fig. 2c) and polar polyenic, or quinonic (Fig. 2d) forms permits the alternating formation of the three single bonds (n)-sandwiched between the indolinium and phenoxide-rings (Fig. 2e). Concomitant rotation about these three single bonds can potentially result in the formation of 2^n theoretical stereoisomers. Whilst some of these isomers are clearly more thermodynamically stable than others, the isomer formed after initial cleavage of the spirocyclic carbon-oxygen bond, or immediately prior to cyclisation, must, skeletally, be that depicted in Fig. 3 (l)—which has support [24]. Previous reports also enforce the theoretical presence of eight potential isomers—four *transoid*- and four *cisoid*-forms; with the relatively high energy *cis*-forms not significantly proportionally contributing to the overall to the equilibrium isomeric mixture [25]. Therefore, the isomers of relatively higher importance in the photochromic process are those possessing a *transoid*-structure.

Considering the observation that the thermal colourisation rate plots-for all four compounds-appear to deviate from linearity would seem to indicate the existence of a more complex ring-opening scenario, as compared against the log rate decolourisation plots for some of the same compounds discussed earlier. Thus, in the case of colourisation it is postulated that one or more of the intermediate mesomeric isomers-depicted in figs f-m below-are implicated to a relatively greater extent. The existence of one or

Table 3
Summary of thermal colourisation kinetic data for compounds **2**, **3**, **4** and **5** in methanol at 21 °C in methanol.

Structure	k_2 (min^{-1})
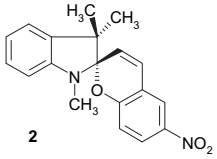 **2**	2.0×10^{-2}
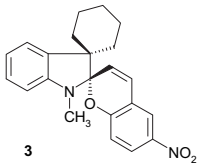 **3**	1.9×10^{-1}
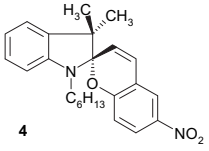 **4**	5.0×10^{-2}
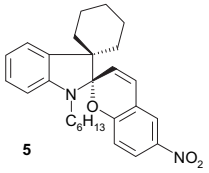 **5**	2.6×10^{-2}

more intermediate mesomeric isomers would probably indicate they possess a relatively increased thermodynamic stability, and hence possess a longer transient lifetime. This postulation can be reinforced since there have been previous literature reports of non-linear plots [26]. In these instances their non-linearity was ascribed to the existence of short and long-lived transient intermediates which were attributed to '*fast and slow fading-rates*'. Further, these non-linear plots have subsequently been resolved into slow and fast-fading first-order rates. The above discussion perhaps explains why, in these particular cases, a slight deviation from a typical linear rate plot is observed.

We subsequently considered the reverse process of thermal decolourisation for compounds **2**, **3**, **4** and **5** under identical physical parameters. The results are summarized below in Graphs 13 and 14 and Table 4 below Graph 15 and 16.

Following the log concentration plots, and determination of the colourisation (k_2) and decolourisation (k_1) rates, enabled calculation of the equilibrium constants K ($=k_2/k_1$) for compounds **2**, **3**, **4** and **5**—for the overall colourisation reaction.

2.5. Thermal decolourisaton rates (k_1)

The rates of thermal decolourisation (ring-cyclisation rate-k_1) for compounds **2**, **3**, **4** and **5** in methanol at 21 °C are 1.6×10^{-2}, 5.5×10^{-2}, 8.4×10^{-2} and 6.9×10^{-2} min^{-1} respectively; which are all of the same order of magnitude. These produce the increasing thermal decolourisation rate trend depicted below:

$$4 > 5 > 3 > 2$$

Two observations become immediately noticeable: 1); the N-hexyl groups promote ring-cyclisation over their equivalent N-methyl substituted compounds as both **4** and **5** possess higher decolourisation rates; and 2) the general increase in steric bulk, through alkyl-substituent does not lead to a general increase in decolourisation rate *e.g.* the more highly substituted 3,3′-cyclohexyl-N-hexyl-substituted compound **5** possesses a slower rate than its equivalent *gem*-dimethyl- congener **4**. However, to the contrary, this is true for the N-methyl-substituted compounds **2** and **3** which would indicate a more complex scenario than simply the position and degree of alkyl-substitution.

The maximal decolourisation rate is noted for the 3,3′-*gem*-dimethyl-N-hexyl derivative **4**, being approximately 22% higher than its 3,3′-cyclohexyl-N-hexyl-substituted congener **5**. In this case it is probable that the steric bulk associated with the 3,3′-cyclohexyl-group relatively promotes ring-opening to the merocyanine over that of *gem*-dimethyl-substituted compound **4**. Thus it is thermodynamically more favorable to remain in the open-form, hence the lower rate of ring-closure (decolourisation). It is, alternatively, and perhaps additionally possible that the merocyanine of compound **4**, being relatively more planar than **5** is able to exist or form an initial micelle-type structure—originating around the n-hexyl grouping. This partly prevents solvation stabilization by the methanol, thus increasing its rate of intramolecular cyclisation. If not quite a micelle-type structure then the more planar merocyanine, possessing long N-hexyl-chains, could lie in a slightly staggered and stacked layer-like structure. The zwitterionic moieties could additionally lie in a planar orientation, but with the iminium and phenoxide ionic charges of each zwitterion lying in such way that each molecules alternate counter-ions are matched and paired. Additionally, there would be Van der Waal's bonding between the layers of hexyl-chains. Overall this structure could, similarly, relatively promote intramolecular ring-cyclisation (decolourisation), by, again, inhibiting the ability of the methanol molecules to solvate the associated zwitterionic charges. In the case

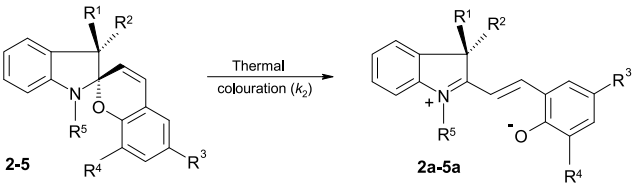

2 $R^1=R^2=CH_3$, $R^3=NO_2$, $R^4=H$, $R^5=CH_3$
3 R^1 / R^2=cyclohexyl, $R^3=NO_2$, $R^4=H$, $R^5=CH_3$
4 $R^1=R^2=CH_3$, $R^3=NO_2$, $R^4=H$, R^5=N-C_6H_{13}
5 R^1 / R^2=cyclohexyl, $R^3=NO_2$, $R^4=H$, R^5=N-C_6H_{13}

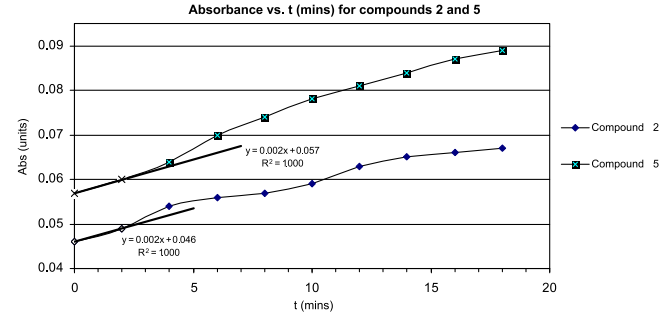

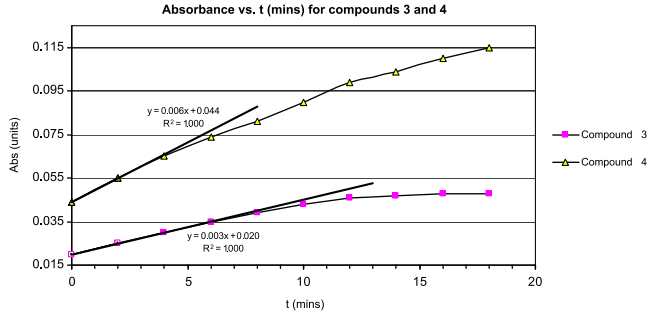

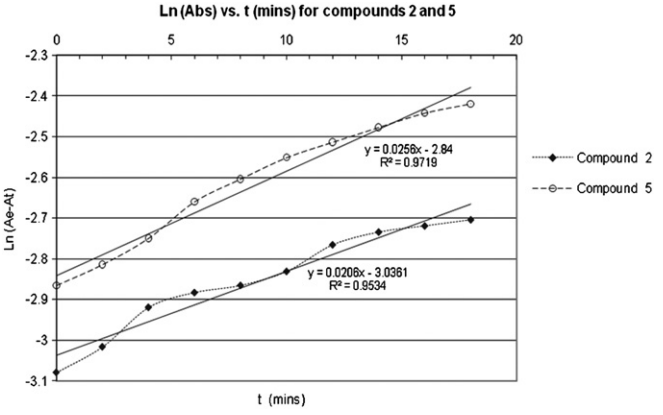

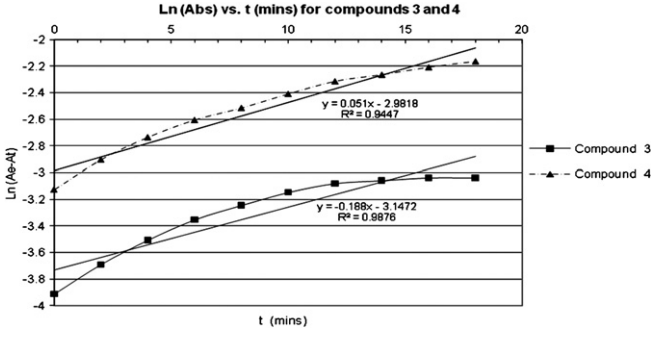

Graphs 13–16. Thermal colourisations (Graph 13 and Graph 14) and log absorbance (Graphs 15 and 16) of compounds **2**, **3**, **4** and **5** in methanol at a concentration of 2×10^{-4} M at 21 °C against time (note: the four compounds had to be represented on two different graphs due to the scale).

Table 4
Summary of thermal decolourisation kinetic data for compounds for **2**, **3**, **4** and **5** at 21 °C in methanol.

Structure	k_1 (min^{-1})
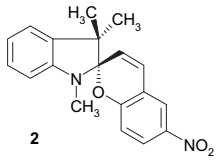 **2**	1.6×10^{-2}
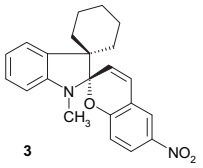 **3**	5.5×10^{-2}
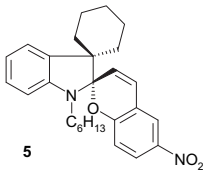 **5**	7.0×10^{-2}
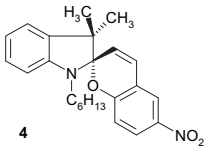 **4**	8.4×10^{-2}

Table 5
Determination of the equilibrium constants (K) for compounds **2**, **3**, **4** and **5** in methanol at 21 °C for the overall colourisation reaction.

Structure	Colouration k_2 (min^{-1}) (previous tables)	Decolouration k_1 (min^{-1}) (previous tables)	K (Cal'd from (k_2/k_1))
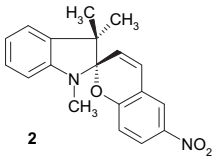 **2**	2.1×10^{-2}	1.6×10^{-2}	1.31
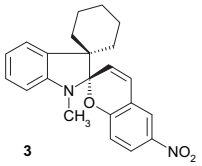 **3**	1.9×10^{-1}	5.5×10^{-2}	3.45
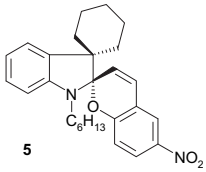 **5**	5.0×10^{-2}	7.0×10^{-2}	0.71
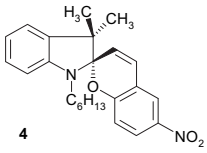 **4**	2.6×10^{-2}	8.4×10^{-2}	0.31

of its 3,3′-cyclohexyl-substitued congener it is probable that the extra steric bulk associated with the cyclohexyl group (which would be expected to sit in the relatively, spatially expansive, open chair- conformation) would prevent, or greatly inhibit these types of effects. The resulting structure would thus be more open and therefore exposed to stabilizing solvent interactions (polar and hydrogen bonding), which would reduce its relative rate of decolourisation (Graph 17–20).

The merocyanine of the N-methyl-3,3′-cyclohexyl-substitued compound **3** possesses a zwitterionic structure which is more stable in methanol than its N-hexyl equivalent **5** (rates of decolourisation: 5.5×10^{-2} (**3**) *vs.* 7.0×10^{-2} min^{-1} (**5**)). This is probably due to the simple fact that it is more polar and hydrogen bond solvated, the latter exerting the greatest effect on decolourisation rates. Again, as discussed above, the larger degree of steric bulk associated with **5**, relative to compound **3**, limits the degree of solvent interactions. Also, the molecule might be expected to form a 'lipophilic shell' which would encourage intramolecular cyclisation to a relatively larger degree than that of **3**.

The slowest decolourisation rate, and by the largest factor (3.4 times), is observed for the least alkyl-substituted compound **2**. This is probably due to the fact that its zwitterionic structure is the most relatively solvated, and hence solution (methanol) stable, of all the four compounds considered herein. It is also likely that the N-alkyl group, being either a methyl or an *n*-hexyl, makes less relative difference to the ring-closure rate. This is because the N-alkyl-during the ring-closing transition state-can undergo pyramidal inversion relieving steric inhibition of phenoxide attack at the base of the iminium-ion's carbon atom (Graph 21).

2.6. Thermal colourisation rates k_2

The rates of thermal colourisation (ring-opening) k_2 for compounds **2**, **3**, **4** and **5** in methanol at 21 °C are 2.1×10^{-2}, 1.9×10^{-1}, 2.6×10^{-2} and 5.0×10^{-2} min^{-1} respectively; which, as opposed to the above decolourisation rates, exhibit a difference in the order of magnitude for one structure (**3**). These compounds produce the increasing thermal colourisation rate trend depicted below:

$$3 > 5 > 4 > 2$$

Some clear observations are noted. The 3,3′-cyclohexyl-substituted compounds **3** and **5** undergo a faster ring-opening than their *gem*-dimethyl substituted structural equivalents **4** and **2**-approximately 9 times faster in the case of **3**, and 2.4 times in the case of **5**. In this case it is likely that the additional steric bulk of the cyclohexyl-substitution promotes ring-opening (colourisation) with the resulting relief in steric strain acting as the intramolecular driving force. Compound **5**, in comparison to compound **3**, additionally possesses an N-hexyl group. This N-hexyl substitution results in a colourisation rate approximately 4 times slower than compound **5** (0.19 min^{-1} (**3**) *vs.* 0.05 min^{-1} (**5**)). The slower rate of colourisation, due to N-alkyl substitution, may arise from the increased steric bulk of the open-form which reduces solvation (methanol) stabilization relative to the less alkyl-substituted structure (**3**).

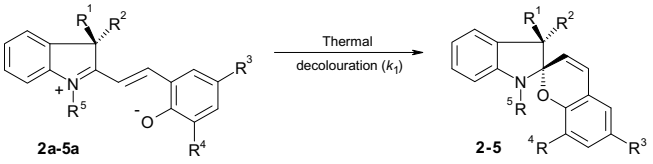

2 $R^1=R^2=CH_3$, $R^3=NO_2$, $R^4=H$, $R^5=CH_3$
3 R^1/R^2=cyclohexyl, $R^3=NO_2$, $R^4=H$, $R^5=CH_3$
4 $R^1=R^2=CH_3$, $R^3=NO_2$, $R^4=H$, R^5=N-C_6H_{13}
5 R^1/R^2=cyclohexyl, $R^3=NO_2$, $R^4=H$, R^5=N-C_6H_{13}

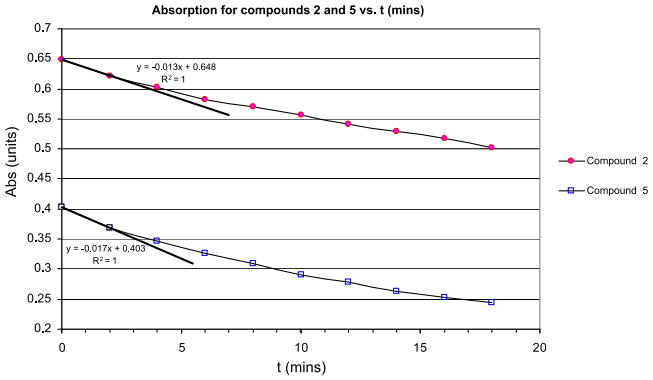

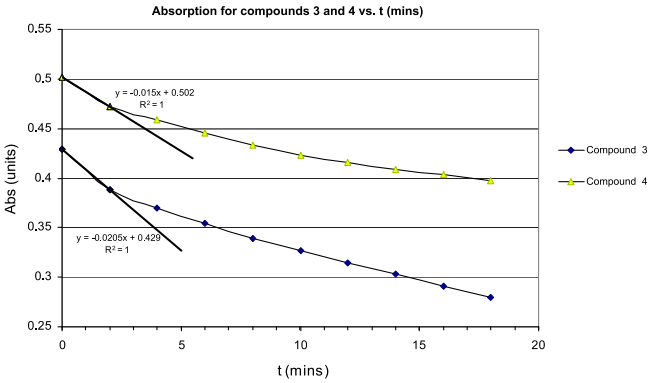

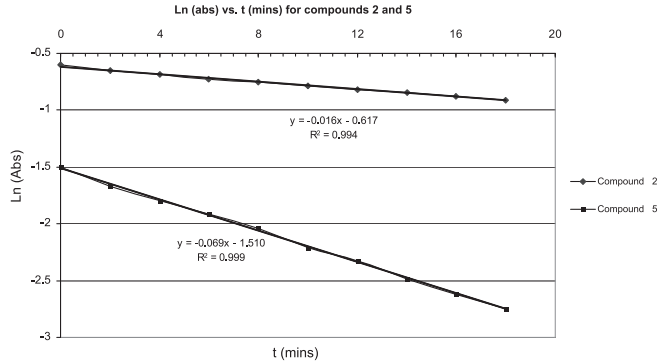

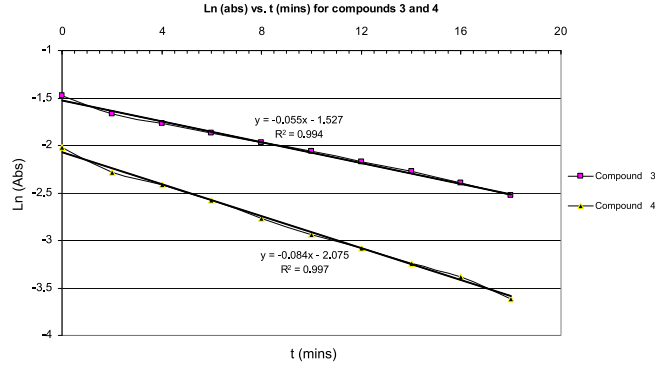

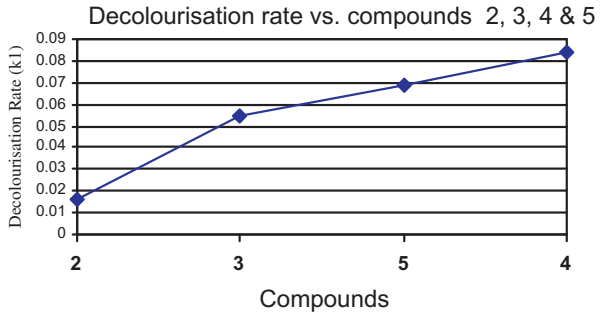

Graph 21. Rate of thermal decolourisations (k_1) plotted against their corresponding compounds; **2**, **3**, **4** and **5** in methanol at 21 °C.

The ring-opening steric effects exerted by the 3,3′-cyclohexyl grouping clearly outweigh that of the reduced solvent stabilization, due to the N-hexyl group, as **5** possesses a decolourisation rate of approximately twice that of **4**—both structures possessing N-hexyl groups. On a reduced solvation, due to the alkyl- substitution argument, **5** would be expected undergo colourisation slower than **4**, however the reverse is true. This verifies the greater effect on ring-opening is steric, and exerted by the 3,3′-cyclohexyl group. This is also vindicated when comparing structures **3** and **2**, differing only in structure by the virtue of a 3,3′-cyclohexyl moiety *vs*. a *gem*-dimethyl substitution. Here the solvation effect differences affected by the N-hexyl groups are negated and emphasise the magnitude of the steric effects induced on substitution of the 3,3′-cyclohexyl-group. This produces a colourisation rate 9 times faster than the *gem*-dimethyl substituted structure **2**. Structure **4** possesses the third fastest colourisation rate (2.6×10^{-2} min^{-1}), and is 1.2 times faster than **2**—the least alkyl-substituted compound. The difference is relatively small when compared to the other observed differences and is probably, in the main, due to an N-hexyl solvation stability effect. This is because the N-hexyl group substitution is unlikely to sterically greatly affect the course of the ring-opening reaction, particularly as pyramidal inversion through the nitrogen atom can partially relieve experienced steric strain.

In summary the ring-opening process is complicated and multifactorial, however the gross observed trends can be suitably explained (Graph 22).

2.7. Equilibrium constants (K)

The equilibrium constants (K—defined here as k_2/k_1) for compounds **2**, **3**, **4** and **5** in methanol at 21 °C are: 1.3, 3.45, 0.31 and 0.71 respectively. This enables establishment of the order depicted below:

$$3 > 2 > 5 > 4$$

Examination of the structures (see overleaf) and relating them to their equilibrium constants enables one to acknowledge some clear trends, and to draw some firm and practically useful conclusions.

Both N-methyl substituted compounds **3** and **2** possess similarly relatively high equilibrium constants (3.46 and 1.31 respectively). In contrast, both N-hexyl substituted compounds **5** and **4** possess similar, but significantly relatively lower equilibrium constants (0.71 and 0.31 respectively) (Graph 23).

Graphs 17–20. Thermal decolourisations (Graphs 17 and 18) and log absorbance (Graph 19 and 20) of compounds **2**, **3**, **4** and **5** in methanol at a concentration of 2×10^{-4} M at 21 °C against time.

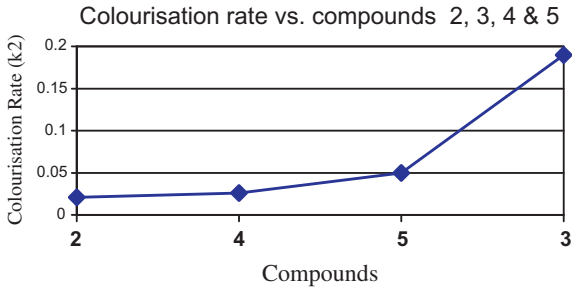

Graph 22. Rate of thermal colourisations (k_2) plotted against their corresponding compounds; **2**, **3**, **4** and **5** in methanol at 21 °C.

The trends within the N-methyl and N-hexyl-substituted series follow a pattern in that in both cases the equilibrium constants for the 3,3′-cyclohexyl-substituted compounds are correspondingly higher than their *gem*-dimethyl congeners *i.e.* 3.35 (**3**) *vs.* 1.31 (**2**) (a ratio of 2.6) and 0.7 (**5**) *vs.* 0.31 (**4**) (a ratio of 2.6) respectively. The ratios exhibit remarkable similarity, indicating a 'constant effect' on substitution of a cyclohexyl group for a *gem*-dimethyl. This is probably due to the significant relief in steric strain, present in the sterically crowded cyclohexyl-substituted closed-forms, obtained on ring-opening (in a methanolic solution at 21 °C).

The fact that there is such a relatively large difference between the N-hexyl and N-methyl-substituted compounds indicates that there is, potentially, at least one particularly important additional factor operating. For example, the equilibrium constant of the N-methyl-3,3′-cyclohexyl substituted compound **3** ($K = 3.45$) is almost 5 times that of the N-hexyl-3,3′-cyclohexyl substituted compound **5** ($K = 0.71$). This could possibly be due to the fact that the more highly alkyl-substituted N-hexyl derivative exhibits reduced solvation stabilization of the zwitterion, due to the increased steric bulk associated with this group. It is also possible that the closed-form of **5** is generally relatively more lipophilically stable-through the operation of Van der Waal's bonding (being more highly alkyl-substituted)-as compared to the closed-form of the corresponding N-methyl congeners. Similar observations are also noted for the compounds **2** ($K = 1.31$) and **4** ($K = 0.31$), the ratio in this case being 4.2 times, remarkably similar, and enforcing the trend noted for compounds **3** and **5**.

3. Summary and conclusions

The thermal decolourisation rate of the 3,3′-cyclohexyl-substituted spirocyclic-compound **3** is greater than that of the simple *gem*-dimethyl-substituted spirocyclic-compound **2**. This trend is consistent in dichloroethane and acetonitrile solvents, but not methanol where the rates are similarly low—this is probably due to a combination of solvation, and particularly hydrogen bonding, which creates a 'rate-levelling effect'. In general, the more polar the solvent, the slower the rate of merocyanine decolourisation. An increase in the temperature (methanol at 50 °C) was accompanied by a faster rate (k_1) of decolourisation (ring-cyclisation)—almost an order of magnitude-for both compounds **3** (1.4×10^{-1} *vs.* 1.0×10^{-2}) and **2** (1.2×10^{-1} *vs.* 2.0×10^{-2}).

The thermal decolourisation of both N-hexyl-substituted compounds **4** and **5** occurs faster than the N-methyl substituted compounds **2** and **3** indicating relative instability of the merocyanine forms; or increased relative thermal stability of the corresponding spirocyclic structures, in methanol (lower solvation stability due to greatly increased alkyl-substitution).

The rates of thermal colourisation were significantly dominated by substitution of a 3,3′-cyclohexyl group which, through the release of steric strain, drove the ring-opening reaction. In this case the N-hexyl-substitutions produced relatively decreased effects. Explanations have been postulated for these observed trends.

In several instances the experimentally determined log rate *vs.* time plots exhibited notable deviations from the expected linearity of unimolecular, or first-order, kinetics. This indicates the occurrence of fast and slow fading-rates strongly suggesting the presence of several intermediate merocyanine isomers. Previous reports have confirmed these observations and resolved the kinetics into fast and slow fading first-order reaction rates.

This has, in the case of several of the spirobenzopyrans discussed herein, been offered as an explanation for the slight deviation from non-linear plots (overall correlation coefficients exhibited a range of 0.94 to ~ 0.99).

Examination of the equilibrium constants (K) reveal a clear trend which enables one to predict how substituent effects may bias and influence the overall equilibria in these systems.

The trend observed in the Gibbs free energy values enforces and parallels that of the equilibrium constants.

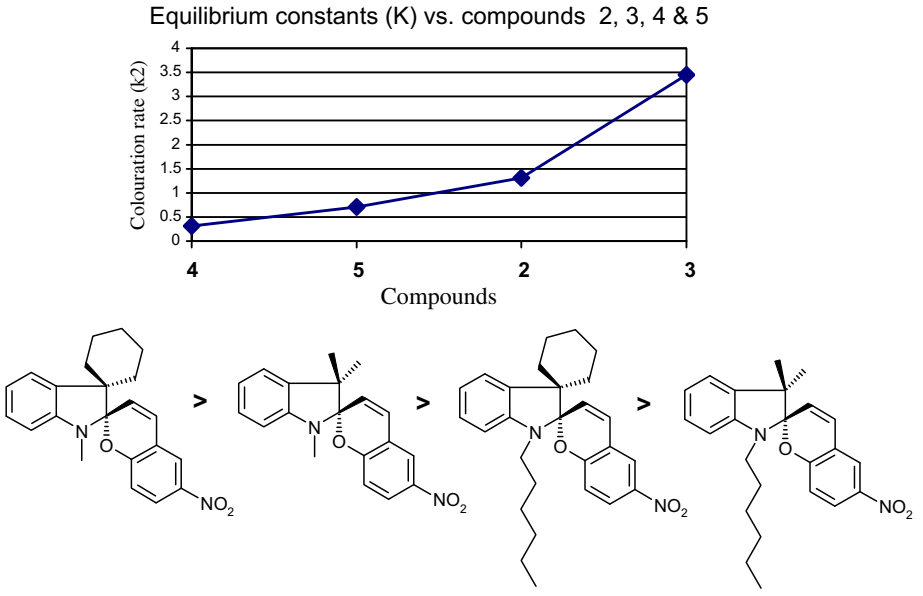

Graph 23. Equilibrium constants (K) for the spirobenzopyran ring-opening ↔ closing reaction plotted against their corresponding compounds; **2**, **3**, **4** and **5** in methanol at 21 °C.

To conclude, the above clearly demonstrates the thermodynamic control that appropriate functional group substitutions can exert on the spirobenzopyran ring-opening ↔ closing reaction, and their magnitude. Additionally, significant and predictable solvent effects are observed, which in turn can be practically used to bias the equilibrium position within these systems. Further, changes in temperature also allow one to bias the concentrations of spirobenzopyran and/or zwitterionic forms. Overall, the above physical parameters, and variations of, allows one to significantly influence and control the interconversion of these systems - obviously important in the design of clean on ↔ off ionic spirobenzopyran-based switches-when required. Ultimately, establishment of how these physical parameters can qualitatively and quantitatively influence the equilibrium position within these systems is extremely important. Further, this methodology can potentially be transferred, incorporated and applied into the design of on ↔ off ionic switches, and *e.g.* ion-chelating systems, including those that additionally possess lariat-type ether appendages *etc*, –a very useful ability.

4. Experimental section

4.1. Photoirradiation studies

The photochromic properties of these compounds were evaluated by preparing solutions (2×10^{-5} mol dm^{-3} unless otherwise stated), in the 'dark', in freshly dried and redistilled solvents (generally acetonitrile, dichloroethane (DCE) or methanol). Perchlorate salts were dried over P_2O_5 for several days before use. Solutions were placed in a stoppered 10 mm pathlength cuvette at room temperature (20–25 °C) and allowed to equilibrate for 1 h before measurement of their UV/Vis absorption curves ('dark' curves). The solutions were then irradiated for 1 min with UV light of $\lambda = 365$ nm generated from a steady power source. The UV light source was a 200 W mercury/xenon lamp, focussed in a LOT-Oriel air-cooled lamp housing, with solution filters[1] to eliminate light of $400 > \lambda > 320$ nm (this allows photoirradiation with a λ_{max} centered at 365 nm, the absorption wavelength of the spirobenzopyrans, and additionally avoids photoirradiation of the formed merocyanine, which has a λ_{max} centered at 550 nm). The UV absorption spectra (UV curve) were measured; this was followed by exposure of the cuvette to a visible light source (3 min: 100 W tungsten spotlight) and the UV absorption spectrum remeasured Fig. 1.

Variable solvent and temperature Studies using UV Spectroscopy.

4.1.1. Thermal decolourisation

The thermal decolourisation of the compounds at 1×10^{-4} M in acetonitrile, DCE and methanol was observed principally after solutions had been irradiated with the UV lamp for 1 min. Immediately after photoirradiation the progressively decreasing merocyanine concentration/absorbance at $\sim\lambda = 550$ nm was continuously monitored, at 21 °C (also at 50 °C for methanol), against time.

Freshly prepared 1×10^{-4} M solutions of the compounds were prepared in the dark (allowing pre-photoirradiation equilibration) in the following solvents: (a) acetonitrile (b) DCE and (c) MeOH.

Specifically, the position of the equilibria were measured using UV spectroscopy adopting the following protocol:

(a) The solutions were left to pre-equilibrate for 1 h in the dark prior to photoirradiation.
(b) The solutions were then exposed to UV light using a focused 200 W high pressure mercury–xenon light source, for 1 min-promoting formation of the merocyanine form.
(c) Continuous measurement of the reducing merocyanine concentration/absorption at ($\lambda = 550$ nm) was undertaken.

4.1.2. Thermal colourisation

The thermal colourisation process of the compounds at 1×10^{-4} M in methanol were observed principally after the solutions had been irradiated with visible light for 3 min (promoting formation of the closed-from). Immediately after photoirradiation the progressively increasing merocyanine concentration/absorbance at $\sim\lambda = 550$ nm was continuously monitored, at 21 °C against time.

Freshly prepared 1×10^{-4} M solutions of the compounds were prepared in the dark (allowing pre-photoirradiation equilibration).

Specifically, the position of the equilibria were measured using UV spectroscopy adopting the following protocol:

(a) The solutions were left to pre-equilibrate for 1 h in the dark prior to photoirradiation.
(b) The solutions were exposed to broad band visible light for 3 min–promoting formation of the closed-form.
(c) Continuous measurement of the increasing merocyanine concentration/absorption at ($\lambda = 550$ nm) was undertaken.

Thermal decolourisation and colourisation UV studies on **2**, **3**, **4** and **5**.

Thermal decolourisation rate for compound **3** and compound **2**, compound **4** and compound **5**, in MeOH at 2×10^{-4} M and at 21 °C.

t (min)	Compound **2**		Compound **3**		Compound **4**		Compound **5**	
	Open-form absorbance at 550 nm	Ln A	Open-form absorbance at 550 nm	Ln A	Open-form absorbance at 550 nm	Ln A	Open-form (A)	Ln A
0	0.648	−0.434	0.429	−0.901	0.502	−0.68916	0.403	−0.90882
2	0.622	−0.475	0.388	−0.947	0.472	−0.75078	0.369	−0.99696
4	0.603	−0.505	0.370	−0.994	0.459	−0.77871	0.346	−1.06132
6	0.583	−0.540	0.354	−1.038	0.446	−0.80744	0.327	−1.11780
8	0.57	−0.563	0.339	−1.080	0.433	−0.83702	0.310	−1.17118
10	0.556	−0.600	0.327	−1.120	0.423	−0.86038	0.290	−1.23787
12	0.542	−0.612	0.314	−1.160	0.416	−0.87707	0.278	−1.28013
14	0.53	−0.639	0.303	−1.190	0.409	−0.89404	0.263	−1.33560
16	0.517	−0.670	0.291	−1.211	0.404	−0.90634	0.253	−1.37437
18	0.502	−0.689	0.280	−1.273	0.397	−0.92382	0.244	−1.41059

[1] A 1°M cobalt and copper sulphate solution (1:1) contained within a 2°mm walled Pyrex® glass cuvette was prepared: This dual combination of a solution and a glass filter possesses an irradiation window between 320-400°nm, with unwanted wavelengths outside this range effectively filtered out.

Thermal colourisation rate for compound **3** and compound **2**, compound **5** and compound **4**, in MeOH at 2×10^{-4} M and at 21 °C.

t (min)	Compound **2**		Compound **3**		Compound **4**		Compound **5**	
	Open-form absorbance at 550 nm	Ln A	Open-form absorbance at 550 nm	Ln A	Open-form absorbance at 550 nm	Ln A	Open-form absorbance at 550 nm	Ln A
0	0.046	−3.07911	0.02	−3.67	0.044	−3.005	0.057	−2.8647
2	0.049	−3.01593	0.025	−3.6	0.055	−2.90042	0.06	−2.81341
4	0.054	−2.91877	0.03	−3.50656	0.065	−2.73337	0.064	−2.74887
6	0.056	−2.8824	0.035	−3.35241	0.074	−2.60369	0.07	−2.65926
8	0.057	−2.8647	0.039	−3.24419	0.081	−2.51331	0.074	−2.60369
10	0.059	−2.83022	0.043	−3.14656	0.09	−2.40795	0.078	−2.55105
12	0.063	−2.76462	0.046	−3.07911	0.099	−2.31264	0.081	−2.51331
14	0.065	−2.73337	0.047	−3.05761	0.104	−2.26336	0.084	−2.47694
16	0.066	−2.7181	0.048	−3.03655	0.11	−2.20727	0.087	−2.44185
18	0.067	−2.70306	0.048	−3.03655	0.115	−2.16282	0.089	−2.41912

The thermal decolourisation and colourisation processes of the four series were studied at 1×10^{-4} M in methanol and measured at 21 °C, versus time.

4.2. Chemical syntheses

^{1}H NMR assignments were carried out with a JEOL FX2000 spectrometer using deuteriochloroform, [D_6]dimethyl sulfoxide or 1,1,2,2-tetrachloroethene (TCE) as the solvent with tetramethylsilane (TMS) as the internal reference. Multiplicities are reported as (s) singlet, (d) doublet, (t) triplet, (q) quartet and (m) multiplet. Assignments of hydroxyl and ammonium protons were verified by deuterium exchange. Mass spectra were recorded with a VG 7070H mass spectrometer interfaced with a Finnegan Incos data system. Accurate mass measurements were carried out at the EPSRC mass spectrometry service at the University of Wales, Swansea. UV spectroscopy was carried out using Perkin–Elmer Lambda 5 and Lambda 9 spectrometers; both instruments are double beamed with thermostatically controlled cell blocks. The Lambda 9 is additionally fitted with as RS 232 port, which allows remote control by PC. All UV measurements were taken at 25 °C using 3 ml quartz cells with a 1 cm path length and are referenced against air. IR spectra were recorded with a Perkin–Elmer 983 spectrometer. Melting points were determined in open capillary tubes with an Electrothermal melting point apparatus and are uncorrected. Elemental analyses were carried out in-house. Thin-layer chromatography was performed over glass plates coated with Merck silica gel 60 F254; flash chromatography was performed using Merck 7734 silica gel (20–63 μm).

Chemical intermediates were purchased from the Aldrich Chemical Company unless otherwise stated.

4.2.1. Syntheses of spirobenzopyrans

6-Nitro-1′,3′,3′-trimethylspiro-[2*H*-1-benzopyran-2,2′-indoline **2**. 1,3,3-Trimethyl-2-methylene indoline (2.50 g, 14.4 mmol) was added to a solution of 2-hydroxy-5-nitrobenzaldehyde (2.42 g, 14.4 mmol), in ethanol (75 mL), and heated under reflux for 8 h. After this period the solution was reduced to approximately one-quarter of its volume, and cooled to 0 °C, whereupon a yellow crystalline solid formed. The solid was filtered off and recrystallised from ethanol to yield the title compound as golden yellow crystals (4.13 g, 89%). mp 178–179 °C. Lit 177–178 °C [27]. δ_H ($CDCl_3$) 7.92 (1H, d, ArH $J = 2$), 7.89 (1H, s, ArH), 7.13 (1H, *t*, ArH $J = 8,2$), 6.99 (1H, d, ArH $J = 7$), 6.83 (1H, d, CH = CH $J = 10$), 6.78 (1H, *t*, ArH $J = 8, 2$), 6.70 (1H, d, ArH $J = 8$), 6.4 (1H, d, ArH $J = 7$), 5.80 (1H, d, CH = CH $J = 10$), 2.70 (3H, s, N–CH_3), 1.30 (3H, s, ArCCH_3), 1.2 (3H, s, ArCCH_3'). $\nu_{(max)}$ ($CDCl_3$)/cm^{-1} 3080, 2980 (sat C–H), 1660, 1615 (C=C), 1575, 1500 (NO_2), 1340 (C–O), 1200 (C–N), 1100 (C–C), 954 (C–O spiro). M/e 322 (M^+, 82.6), 292 (9.2), 261 (14.5), 217 (8.6), 159 (base peak 100%).

1′-Methyl-6-nitro-3′spirocyclohexylspiro-[2*H*-1-benzopyran-2,2′-indoline] **3**. 1,2-Dimethyl-3-spirocyclohexyl indolium triflate (1.02 g, 2.81 mmol) was dissolved in a 40% sodium hydroxide solution (10 mL) and the resulting solution stirred for 5 min. Diethylether (15 mL) was added to the stirred solution and after 5 min separated from the reaction mixture, dried (anhydrous sodium sulphate) and evaporated under reduced pressure. The yellow/orange oil that resulted was isolated (0.4 g, 1.87 mmol), dissolved in ethanol (3 mL), added to 2-hydroxy-5-nitrobenzaldehyde (0.31 g, 1.87 mmol) in ethanol (10 mL), and the resulting solution heated under reflux for 24 h. The ethanol was reduced in volume to approximately one-quarter, under reduced pressure, and left overnight at 0 °C whereupon a slightly brown solid formed. The solid was filtered off and recrystallised from ethanol to yield the title compound as a tan coloured precipitate (0.37 g, 55%). mp 122–124 °C. δ_H ($CDCl_3$) 8.02 (1H, d, ArH $J = 2$), 7.99 (1H, s, ArH), 7.44, 7.42 (1H, d, ArH), 7.26 (1H, s, ArH), 7.24, 7.20 (1H, *t*, ArH), 6.9 (1H, s, ArH), 6.84–6.88 (1H, *t*, ArH), 6.74–6.76 (1H, d ArH $J = 8$), 6.58–6.55 (1H, d, ArH), 5.88–5.90 (1H, d, ArH $J = 10$), 2.7 (3H, s, N–CH_3), 1.97–1.31 (10H, m, cyclohexyl 5 × CH_2). $\nu_{(max)}$ ($CDCl_3$)/cm^{-1} 2936, 3020 (sat C–H), 1608 (C=C), 1516 (C=N), 1338, 1450 (NO_2), 1216 (C–N), 1088 (C–C), 954 (C–O spiro), 775 (ArH, 4 adj H's). M/e 363 (M^++1, 23.6), 362 (M^+, 65.0), 361 ($M^+ - 1$, 5.1), 83 (base peak 100%). (Found: C 72.71, H 6.05, N 7.48. $C_{22}H_{22}N_2O_3$. requires C 72.91, H 6.12, N 7.73).

1′-Hexyl-6-nitro-3′,3′-dimethylspiro-[2*H*-1-benzopyran-2,2′-indoline] **4**. 3,3-Dimethyl-1-hexyl-2-methyl indolium iodide (0.91 g, 2.45 mmol) was dissolved in a stirred 40% sodium hydroxide solution (30 mL). Following this, diethylether (100 mL) was added and the mixture vigorously stirred for 15 min. After this period the diethylether layer was separated, dried (anhydrous sodium sulphate), filtered and evaporated under reduced pressure to yield an yellow/orange oil (0.38 g, 1.56 mmol): this oil was isolated, added to 2-hydroxy-5-nitrobenzaldehyde (0.26 g, 1.56 mmol) in ethanol (15 mL), and the resulting solution heated under reflux overnight. Partial (approximately 75%) evaporation of the solvent under reduced pressure, followed by overnight refrigeration, produced a solid which was broken up and recrystallised from chloroform:hexane (1:1) to yield the title compound as a dusty pink solid (390 mg, 64%). mp 104–106 °C. δ_H ($CDCl_3$) 8.02 (1H, d (obs), ArH $J = 7$), 7.99 (1H, d, ArH $J = 7$), 7.16–7.20 (1H, *t*, ArH $J = 7$), 7.06, 7.08 (1H, d, ArH $J = 8$), 6.88 (1H, d, CH = CH $J = 10$), 6.85–6.90 (1H, *t*, ArH $J = 7$), 6.73–6.75 (1H, d, ArH $J = 8$), 6.56, 6.58 (1H, d, ArH $J = 8$), 5.85, 5.87 (1H, d, CH = CH (*cis*) $J = 10$), 3.11–3.25 (10H, m, 5 × -CH_2), 1.18–1.28 (6H, 2× s, *gem* –C(CH_3)$_2$), 0.83–0.87 (3H, *t*, hexyl-CH_3). $\nu_{(max)}$ ($CDCl_3$)/cm^{-1} 2856, 2932 (sat C–H), 1610 (C=C), 1472 (C–O), 1336 (NO_2), 1274 (C–N), 1090 (C–C), 954 (C–O spiro), 732 (ArH, 4 adjacent H's). M/e 392 (M^+, 7.6), 172 (base peak, 100%). $C_{24}H_{28}N_2O_3$ Acc. (EI) requires: 392.2100 Found: 392.2100.

1′-Hexyl-6-nitro-3′-spirocyclohexylspiro-[2*H*-1-benzopyran-2,2′-indoline] **5**. 1-Hexyl-2-methyl-3-spirocyclohexyl indolium iodide (0.79 g, 1.92 mmol) was dissolved in a 40% sodium hydroxide solution (30 mL) by vigorously stirring. Following this, diethylether (100 mL) was added and the solution vigorously stirred for 15 min: After this period the diethylether layer was separated from the reaction mixture, dried (anhydrous sodium sulphate) and evaporated under reduced pressure to yield an orange oil (0.36 g, 1.27 mmol). The oil was isolated, added to 2-hydroxy-5-nitrobenzaldehyde (0.21 g, 1.26 mmol) in ethanol (15 mL) and the resulting solution refluxed overnight. After this period the solution was allowed to cool, the ethanol reduced in volume to approximately 5 mL and the resulting mixture left in a refrigerator overnight. The solid that formed was filtered off and recrystallised from chloroform: hexane (1:1) to yield the title compound as a dusty pink solid (300 mg, 55%). mp 122–124 °C. δ_H ($CDCl_3$) 7.99, 8.01 (1H, d (obscured), $J = 9$, ArH, $J = 9$), 7.99 (1H, s, ArH), 7.41, 7.43 (1H, d, Ar $J = 7$), 7.21 (1H, *t*, ArH), 6.86, 6.89 (1H, d, CH = CH, $J = 10$), 6.80–6.89 (1H, *t*, ArH), 6.71–6.71 (1H, d, ArH, $J = 9$), 6.58, 6.58 (1H, d, ArH, $J = 7$), 5.87, 5.90 (1H, d, CH = CH, $J = 10$–*cis*-form), 3.05–3.22 (10H, m, 5 × CH_2), 1.26–1.97 (10H, m, cyclohexyl 5 × CH_2), 0.84–0.86 (3H, *t*, CH_3). $\nu_{(max)}$ ($CDCl_3$)/cm^{-1} 2934, 2856 (sat C–H), 1612 (C=C), 1472 (C–O), 1336 (NO_2), 1276 (C–N), C–C (1090), 954 (C–O spiro), 732 (ArH, 4 adj H's). M/e 433 (M^++1, 37.7), 432 (base peak, 100%) 431 ($M^+ - 1$, 8.8). (Found: C 74.70, H 7.48, N 6.38. $C_{27}H_{32}N_2O_3$ requires C 74.79, H 7.48, N 6.47).

4.2.2. Syntheses of N-alkyl indoles

1-Hexyl-2-methyl-3-spirocyclohexyl indolium iodide. 3-Cyclohexyl-2-methyl-3*H*-indole (1.01 g, 5.09 mmol) and hexyl iodide (1.08 g, 5.09 mmol) were heated under reflux for 24 h. After this period the remaining solution was cooled, yielding the title compound as a deep black/red waxy solid (1.41 g, 68%). mp (formed a gum). δ_H ($CDCl_3$) 7.94, 7.96 (1H, d, ArH $J = 7$), 7.68, 7.70 (1H, d, ArH $J = 7$), 7.60 (1H, *t*. ArH), 7.57 (1H, *t*, ArH), 4.70 (2H, *t*, N^+–CH_2CH_2), 3.16 (3H, s, $-N^+ = C-CH_3$), 1.23–2.13 (18H, m, 9 × CH_2), 0.91 (3H, *t*, hexyl, $CH_2\underline{CH_3}$). $\nu_{(max)}$ ($CDCl_3$)/cm^{-1} 2930, 3018 (sat C–H), 1600 (C=C), 1126 (C=N), 1216 (C–N), 1042 (C–C), 736 (ArH, 4 adj H's). M/e 285 (M^+ + 2-HI, 7.5), 284 (M^+ + 1-HI, 44.8), 283 (M^+ – HI, 100% base peak), 282 (M^+-1-HI, 20.8). $C_{20}H_{29}N$ Acc. (EI) requires: 283.2300 Found: 283.2300.

3,3-Dimethyl-1-hexyl-2-methyl indolium iodide. 3,3-Dimethyl-2methyl-3*H*-indole (1.00 g, 6.28 mmol) and hexyl iodide (1.39 g, 6.55 mmol) were heated under reflux for 24 h. The solid that formed was broken up and washed with diethylether to yield the title compound as a deep red powder (1.21 g, 51%). mp (formed a 'gum'). δ_H ($CDCl_3$) 8.52–8.55 (4H, m, ArH), 4.66–4.51 (10H, *t*, 5 × CH_2), 3.53 (3H, s, $N^+ = C-CH_3$), 1.18 (6H, 2 × s, *gem* $-C(CH_3)_2$), 0.63 (3H, *t*, hexyl $CH_2\underline{CH_3}$). $\nu_{(max)}$ ($CDCl_3$)/cm^{-1} 2940, 3018 (sat C-H), 1606 (C=C), 1640 (C=N), 1216 (C–N), 1032 (C–C). M/e 243 (M^+ – HI, 50.1), 242 (M^+ – HI, 5.5), 144 (100% base peak).

1,2-Dimethyl-3-spirocyclohexyl indolium triflate. 2-Methyl-3-spirocyclohexyl-3*H*-indole (3.22 g, 16.18 mmol) was added to methyltrifluoromethane sulphonate (2.66 g, 16.22 mmol) in a mixture of hexane (20 mL) and diethylether (30 mL). Instantly, a canary yellow precipitate formed which was filtered off and washed with cold diethylether to yield the title compound as pale yellow crystals (4.59 g, 78%). mp 126–128 °C. δ_H ($CDCl_3$) 7.91, 7.93 (1H, d, ArH), 7.66–7.68 (1H, d, ArH), 7.62 (1H, *t*, Ar $J = 8$), 7.56 (1H, *t*, ArH $J = 8$), 4.12 (3H, s, N^+–CH_3), 2.88 (3H, s, $N^+ = C-CH_3$), 1.54, 2.08 (10H, m, cyclohexyl 5 × CH_2). $\nu_{(max)}$ ($CDCl_3$)/cm^{-1} 3020 (sat C–H), 1590 (C=C), 1325 (C–C), 1210 (C–N), ArH (760), 758 (C–F). M/e 233 (M^+ – (SO_3CF_3), 6.7), 323 (M^+ – SO_3CF_3-1, 41.7), 218 (M^+-SO_3CF_3-15, 17.7), 217 (base peak, 100%) 203 (M^+-SO_3CF_3-2 × 15, 4.2). (Found: C 52.50, H 5.36, N 3.88. $C_{16}H_{20}NO_3F_3S$ requires C 52.88, H 5.55, N 3.86).

4.2.3. Syntheses of indolenines

1-Methyl-3-spirocyclohexyl-2-methylene indolenine. 1,2-Dimethyl-3-spirocyclohexyl indolium triflate (**5.19**) (1.02 g, 2.81 mmol) was dissolved in a 40% sodium hydroxide solution (10 mL) and stirred for 10 min. After this period diethylether (10 mL) was added and the solution stirred for a further 5 min. The diethylether layer was separated from the reaction mixture, dried (anhydrous sodium sulphate), filtered, and removed under reduced pressure to yield the title compound as a yellow/orange oil (0.45 g, 75%). δ_H ($CDCl_3$) 7.44 (1H, d, ArH $J = 7$), 7.14 (1H, *t*, ArH), 6.74 (1H, *t*, ArH), 6.56 (1H, d, ArH $J = 7$), 3.88 (2H, dd, C=CH_2 $J = 10$, 10), 3.02 (3H, s, N–CH_3), 1.83 (10H, m, cyclohexyl 5 × CH_2). $\nu_{(max)}$ ($CDCl_3$)/cm^{-1} 2934 (sat C–H), 1644 (C=N), 1604 (C=C), 1908 (C–C), 908 (C–C), 775 (ArH, 4 adj H's). M/e 215 (M^++1, 18.5), 214 (M^+, 46.9), 213 ($M^+ - 1$, 80.0), 158 (base peak, 100%), 306 ($M^+ - 1$, 15.8). $C_{15}H_{19}N$ Acc. (EI) requires: 213.1517 Found: 213.1517.

4.2.4. Synthesis of 3H-indoles

3-Cyclohexyl-2-methyl-3*H*-indole. Cyclohexylmethyl ketone phenylhydrazone (4.65 g, 21.53 mmol) was added to zinc chloride (1.00 g, 7.35 mmol) in glacial acetic acid (100 mL), and the resulting solution heated on a steam bath, under nitrogen, for 3 h. The resulting solution was cooled to room temperature, filtered, and the remaining glacial acetic acid removed under reduced pressure to yield the title compound as an orange oil (3.25 g, 76%). δ_H ($CDCl_3$) 7.51–7.53 (1H, d, ArH $J = 7$), 7.31 (1H, d, ArH $J = 7$), 7.15, 6.99 (2H, m, ArH), 2.7 (3H, s, N=C–CH_3), 1.25–2.31 (10H, m, cyclohexyl 5 × CH_2). $\nu_{(max)}$ ($CDCl_3$)/cm^{-1} 2932 (sat C–H), 1688 (C=N), 1598 (C=C, Ar), 1216 (C–N), 1026 (C–C). M/e 200 (M^++1, 27.6), 199 (M^+, base peak, 100%), 198 ($M^+ - 1$, 4.2). $C_{14}H_{17}N$ Acc. (EI) requires: 199.1361 Found: 199.1361.

3,3′-Dimethyl-2-methyl-3*H*-indole. A mixture of isopropyl methyl ketone phenylhydrazone (1.69 g, 9.60 mmol) and hydrochloric acid (30 mL) was heated under reflux for 1 h prior to stirring at room temperature for 3 h. After this period the resulting mixture was filtered and the hydrochloric acid removed under reduced pressure to yield a red oil. Column chromatography of the oil over silica using ethyl acetate as the eluent yielded the title compound as a reddish oil (1.19 g, 78%). δ_H ($CDCl_3$) 7.0–7.6 (4H, m, ArH), 2.3 (3H, s, CH_3), 1.3 (6H, s, $ArCH_3$). $\nu_{(max)}$ ($CDCl_3$)/cm^{-1} 3018 (sat C–H), 1450 (C=N), 1533 (C=C), 1210 (C–C), 1190 (C–N), 771 (ArH, 4 adj H's). M/e 159 (M^+, 11.9), 146 (base peak, 100%).

4.2.5. Syntheses of hydrazones

Isopropyl methyl ketone phenylhydrazone. Phenyl hydrazine (1.65 g, 15.28 mmol) was added to 2-methyl-3-pentanone (2.48 g, 24.80 mmol) in ethanol (10 mL) and the resulting solution heated under reflux for 5 h. After this period the ethanol and excess 2-methyl-3-pentanone were removed under reduced pressure (rotary evaporation) to yield title compound as mobile, slightly red oil (3.20 g, 68%). δ_H ($CDCl_3$) 6.8–7.3 (5H, m, ArH), 4.75 (1H, bs, NH), 2.55 (1H, hept, $(CH_3)_2$)C–$\underline{H}$), 1.91 (3H, s, CH_3), 1.14 (6H, d, $(CH_3)_2$C–H). $\nu_{(max)}$ ($CDCl_3$)/cm^{-1} 3300–3500 (=N–H, w, secondary amine), 3100 (C–H), 1650 (C=C), 1530 (C=N).

Cyclohexyl ketone phenylhydrazone [28]. Phenylhydrazine (3.00 g, 27.77 mmol) was added to cyclohexylmethyl ketone (3.50 g, 27.77 mmol) in ethanol (100 mL) and the resulting solution heated under reflux for 0.5 h. Removal of the ethanol under reduced pressure yielded the title compound as a deep orange mobile oil (4.78 g, 79%). δ_H ($CDCl_3$) 11.0 (1H, s, NH, exchangeable D_2O), 7.25 (2H, *t*, ArH), 7.03, 7.05 (2H, dd, ArH), 6.79, 6.83 (1H, *t*, ArH $J = 8$), 1.90 (1H, m, $(CH_2)_2C\underline{H}C$), 1.82 (3H, s, N=C–CH_3), 1.17–1.78 (10H, m, cyclohexyl 5 × $C\underline{H}_2$). $\nu_{(max)}$ ($CDCl_3$)/cm^{-1} 3650 (N–H), 3020 (C–H), 1616 (C=C), 1520 (C–N), 1020 (C–C), 760 (ArH). M/e 216 (M^+, 6.6), 215 ($M^+ - 1$, 8.1), 18 (base peak, 100%).

4.2.6. Syntheses of salicaldehydes

2-Hydroxy-5-nitrobenzaldehyde. Hexamethylenetetramine (1.40 g, 10 mmol) was added in portions, over 15 min, to a stirred mixture of 4-nitrophenol (1.39 g, 10 mmol) in 85% polyphosphoric acid (8 mL). The resulting solution was heated to 100 °C and maintained at this temperature for 2 h. Cold water (40 mL) was added to the stirred solution whilst maintaining the temperature at near to 15 °C by cooling over an ice bath. The solid that formed was filtered off and washed with a little cold water (2 × 25 mL). Drying yielded title compound as a cream coloured solid (0.97 g, 58%). mp 127–129 °C. Lit 128 °C [29]. δ_H (DMSO) 10.35 (1H, s, CHO), 8.42 (1H, br s, ArH), 8.35–8.33 (1H, br d, ArH), 7.17–7.20 (1H, d, ArH). $\nu_{(max)}$ ($CDCl_3$)/cm^{-1} 3682 (OH), 3020 (C–H), 1722 (C=O), 1594 (C=C), 1320 (C–C), 1216 (NO_2). M/e 169 (M^++ 2, 3.0), 168 (M^++1, 23.8), 167 (M^+, base peak 100%).

Acknowledgements

Input from Dr Thomas Nevell (School of Pharmacy and Biomedical Sciences, University of Portsmouth), regarding the interpretation of the kinetic data is gratefully acknowledged.

The authors thank the Science and Engineering Research Council (SERC) for a grant supporting this research.

References

[1] (a) Willner I, Wilner B. Chemistry of photobiological switches. In: Morrison H, editor. Biological applications of photochemical switches. New York: John Wiley & Sons; 1993. p. 1–110;
(b) Winkler JD, Deshayes K, Shao B. Photochemical binding, release and transport of metal ions. In: Morrison H, editor. Biological applications of photochemical switches. New York: John Wiley & Sons; 1993. p. 171–96;
(c) Lukyanov B, Lukyanova M. Spiropyrans: synthesis, properties, and application. Chem Heterocyclic Compounds 2005;41(3):281–311;
(d) Alfimov MV, Fedorova OA, Gromov SP. Photoswitchable molecular receptors. J Photochem Photobiol A Chem 2003;158:183–98.

[2] (a) Inouye M. Coord Chem Rev 1996;148:265–83;
(b) Inouye M, Akanatsu K, Nakazumi H. Chem Commun. 1997;119:9160;
(c) Zhou J, Zhao F, Li Y, Zha F, Song X, Am J. Chem Soc 1995;92:193;
(d) Alfimov MV, Fedorov YV, Fedorova OA, Gromov SP, Hester RE, Lednev IK, et al. J Chem Soc Perkin Trans 1996;2:1441;
(e) Alfimov MV, Churakov AV, Fedorov YV, Gromov SP, Hester RE, Howard AK, et al. J Chem Soc Perkin Trans 1997;2:2249;
(f) Fedorova OA, Strokach YP, Gromov SP, Koshkin AV, Valova TM, Alfimov MV, et al. New J Chem 2002;26:1137.

[3] (a) Bertleson RC. Photochromism [Chapter 3]. In: Brown GH, editor. Techniques of organic chemistry. New York: Wiley Interscience; 1971. p. 45–294;
(b) Guglielmetti R. Photochromism molecules and systems [Chapter 8]. In: Dürr H, Bouas-Laurent H, editors. Amsterdam: Elsevier; 1990. p. 314–466.

[4] (a) Kimura K, Yamashita T, Yokoyama M. J Chem Soc Chem Commun; 1991:147;
(b) Kimura K, Yamashita T, Yokoyama M. J Chem Soc Perkin Trans 1992;2:613.

[5] Kimura K. Coord Chem Rev 1996;148:41.

[6] Kimura K, Kaneshiga M, Yamashita T, Yokoyama M. J Org Chem 1994;59:1521.

[7] Tanaka M, Kamada K, Ando H, Kitagako T, Shibutani Y, Yajima S, et al. Chem Commun; 1999:1453.

[8] Sakata T, Jackson DK, Mao S, Marriott G. J Org Chem 2008;73(1):227–33.

[9] Keum SM, Hur MS, Kazmaie PM, Buncel E. Can J Chem 1991;69:1940–7.

[10] Bertleson RC. Photochromism [Chapter 3]. In: Brown GH, editor. Techniques of organic chemistry. New York: Wiley Interscience; 1971. p. 45–431.

[11] Sheng Y, Leszczynski J, Garcia A, Rosario R, Gusy D, Springer J. J Phys Chem Chem B 2004;108:16235–43.

[12] Kawanishi Y, Seki K, Tamaki T, Sakuragi M, Suzuki Y, Photochem J, et al. Photobiol A 1997;109:237–42.

[13] Roxburgh CJ, Sammes PG. Eur J Org Chem 2006;4:1050–6.

[14] Roxburgh CJ, Sammes PG. Dyes Pigm 1995;28:317–25.

[15] (a) Roxburgh CJ, Sammes PG, Abdullah A. Dyes Pigm 2008;76(2):319–26;
(b) Roxburgh CJ, Sammes PG, Abdullah A. Dyes Pigm 2009;(8):31–50.

[16] Roxburgh CJ, Sammes PG, Abdullah A. Dyes Pigm 2009;82:226–37.

[17] Roxburgh CJ, Sammes PG, Abdullah A. Eur J Org Chem; 2008:4951–60.

[18] Lee IJ, Huh YD. Bull Korean Chem. Soc 1996;17(9):865–8.

[19] Durr H. General introduction. In: Durr H, Bous-Laurent H, editors. Photochromism: molecules and systems. 1.ed, vol 40. Amsterdam: Elsevier Science Publishing House; 1990. p. 1–14.

[20] Li. Y, Zhou J, Jinwei, Wang Y, Zhang F, Song X, .. J Photochem Photobiol A 1998;113:65–72.

[21] Bertelson RC. In: Crano JC, Guglielmetti RJ, editors. Organic photochromic and thermochromic compounds, vol. 1. New York: Plenum; 1999.

[22] Muskegon, MI: Burdick and Jackson Labs, http://macro.lsu.edu/howto/solvents/Polarity%20index.htm; 1980.

[23] Gabbutt CD, Rickwood M, Hepworth JD. and Marsden SD. Eur. Pat. No. 93309418.7. Nov. 1993.

[24] Hobley J, Malatesta V, Millini R, Montanari L, O Neil Parker Jr W. Phys Chem Chem Phys 1999;1:3259.

[25] Heligman Rim R, Hirshberg Y, Fisher E. J Phys Chem 1962;66:2465.

[26] Brown GH. In: Photochromism–techniques of chemistry, vol 3. John Wiley And Sons, Inc.; 1971. p. 1–853.

[27] Bercovici T, Heiligman-Rim R, Fischer E. Mol Photochem 1969;1:189–201.

[28] Lyle RE, Skarlos L. J Chem Soc Chem Commun; 1966:644–6.

[29] (a) Suzuki Y, Takahashi H. Chem Pharm Bul 1983;31(11):1251–753;
(b) Duff JC, Bills EJ. J Chem Soc; 1934:1305;
(c) Ogata Y, Kawasaki A, Gugiura F. Tetrahedron 1968;24:5001. 15.